

PREPROCESSING OF TANDEM MASS SPECTRA  
USING MACHINE LEARNING METHODS

A Thesis Submitted to the  
College of Graduate Studies and Research  
in Partial Fulfillment of the Requirements  
for the degree of Master of Science  
in the Department of Mechanical Engineering  
University of Saskatchewan  
Saskatoon

By  
Jiarui Ding

©Jiarui Ding, 05/2009. All rights reserved.

# PERMISSION TO USE

In presenting this thesis in partial fulfilment of the requirements for a Postgraduate degree from the University of Saskatchewan, I agree that the Libraries of this University may make it freely available for inspection. I further agree that permission for copying of this thesis in any manner, in whole or in part, for scholarly purposes may be granted by the professor or professors who supervised my thesis work or, in their absence, by the Head of the Department or the Dean of the College in which my thesis work was done. It is understood that any copying or publication or use of this thesis or parts thereof for financial gain shall not be allowed without my written permission. It is also understood that due recognition shall be given to me and to the University of Saskatchewan in any scholarly use which may be made of any material in my thesis.

Requests for permission to copy or to make other use of material in this thesis in whole or part should be addressed to:

Head of the Department of Mechanical Engineering  
57 Campus Drive  
University of Saskatchewan  
Saskatoon, Saskatchewan  
Canada  
S7N 5A9

# ABSTRACT

Protein identification has been more helpful than before in the diagnosis and treatment of many diseases, such as cancer, heart disease and HIV. Tandem mass spectrometry is a powerful tool for protein identification. In a typical experiment, proteins are broken into small amino acid oligomers called peptides. By determining the amino acid sequence of several peptides of a protein, its whole amino acid sequence can be inferred. Therefore, peptide identification is the first step and a central issue for protein identification. Tandem mass spectrometers can produce a large number of tandem mass spectra which are used for peptide identification. Two issues should be addressed to improve the performance of current peptide identification algorithms. Firstly, nearly all spectra are noise-contaminated. As a result, the accuracy of peptide identification algorithms may suffer from the noise in spectra. Secondly, the majority of spectra are not identifiable because they are of too poor quality. Therefore, much time is wasted attempting to identify these unidentifiable spectra.

The goal of this research is to design spectrum pre-processing algorithms to both speedup and improve the reliability of peptide identification from tandem mass spectra. Firstly, as a tandem mass spectrum is a one dimensional signal consisting of dozens to hundreds of peaks, and majority of peaks are noisy peaks, a spectrum denoising algorithm is proposed to remove most noisy peaks of spectra. Experimental results show that our denoising algorithm can remove about 69% of peaks which are potential noisy peaks among a spectrum. At the same time, the number of spectra that can be identified by Mascot algorithm increases by 31% and 14% for two tandem mass spectrum datasets. Next, a two-stage recursive feature elimination based on support vector machines (*SVM-RFE*) and a sparse logistic regression method are proposed to select the most relevant features to describe the quality of tandem mass spectra. Our methods can effectively select the most relevant features

in terms of performance of classifiers trained with the different number of features. Thirdly, both supervised and unsupervised machine learning methods are used for the quality assessment of tandem mass spectra. A supervised classifier, (a support vector machine) can be trained to remove more than 90% of poor quality spectra without removing more than 10% of high quality spectra. Clustering methods such as model-based clustering are also used for quality assessment to cancel the need for a labeled training dataset and show promising results.

# ACKNOWLEDGEMENTS

I would express my sincere thanks to my advisor, Professor Fang-Xiang Wu, for supporting me over my study and research over the years. In particular, I would like to thank Professor Wu for introducing me to the fascinating world of Bioinformatics, for giving me the freedom to exploring the new areas, and for helping me with living in a foreign country. I would also like to thank Prof. Wu for his critical yet insightful comments on my publications as well as this thesis. Finally, I would like to thank Professor Wu for reading and editing my publications and thesis so many times. Without his help, it is impossible for me to complete this work.

I would like to thank my committee members: Professor W.J. (Chris) Zhang, Professor Aryan Saadat Mehr, for their valuable examinations and suggestions to improve the present work. I would like to extend my thanks to the professors who have taught me in various graduate courses. They are Mark G. Eramian, Longhai Li, Michael Horsch, Ian McQuillan and Eric Salt. Much knowledge from them has become a part of this thesis. I would like to specially thank Professor Ian McQuillan, who is also my external examiner, for his great comments to improve the mathematical notations and English expressions in this thesis.

I would also like to acknowledge my colleagues and friends for their friendship, discussion and help to make this study a wonderful journey. Special thanks go to Ruizhi Luo, An-Min Zou, Lei Mu, Jinhong Shi, Jian Sun and many others.

I would like to thank Natural Sciences and Engineering Research Council of Canada (NSERC) for financial support to do this research, and the University of Saskatchewan for funding me through a graduate scholarship award.

Finally, I would like to express my deepest gratitude to the people who have supported me all the way to the point where now I am. I would like to thank my sister Yaping Ding for her support during the most difficult times. I would like to thank my parents, Liangzheng Ding and Chengshu Zhang for all they have given me. And at last Chaoxia Lu, that very special person, for all her love, encouragement and dedications!

*This thesis is dedicated to my fiancée:*

*Chaoxia Lu*

# CONTENTS

<b>Permission to Use</b>	<b>i</b>
<b>Abstract</b>	<b>ii</b>
<b>Acknowledgements</b>	<b>iv</b>
<b>Contents</b>	<b>vi</b>
<b>List of Tables</b>	<b>viii</b>
<b>List of Figures</b>	<b>ix</b>
<b>List of Abbreviations</b>	<b>x</b>
<b>1 Introduction and problem description</b>	<b>1</b>
1.1 Background . . . . .	1
1.2 Objectives . . . . .	5
1.3 Spectral pre-processing . . . . .	6
1.4 Overview of the rest of this thesis . . . . .	7
<b>2 Denoising tandem mass spectra</b>	<b>10</b>
2.1 Introduction . . . . .	10
2.2 Methods . . . . .	12
2.2.1 Peak intensity adjustment . . . . .	13
2.2.2 Peak local maximum extraction . . . . .	17
2.3 Results and discussion . . . . .	19
2.3.1 Datasets . . . . .	19
2.3.2 Overall spectrum denoising results . . . . .	20
2.3.3 The functions of each module . . . . .	23
2.3.4 Discussion and further improvement . . . . .	24
2.4 Conclusions . . . . .	27
<b>3 Feature selection for tandem mass spectrum quality assessment</b>	<b>29</b>
3.1 Introduction . . . . .	29
3.2 Feature selection . . . . .	31
3.2.1 Background . . . . .	31
3.2.2 The workflow for selecting the most relevant features . . . . .	34
3.2.3 Local cumulative normalization . . . . .	34
3.2.4 Feature construction . . . . .	37
3.2.5 Feature selection using sparse logistic regression . . . . .	40
3.2.6 Feature selection using SVM-RFE . . . . .	42
3.3 Results and discussion . . . . .	46

3.3.1	Experimental datasets . . . . .	46
3.3.2	Training and performance evaluation . . . . .	47
3.3.3	Feature selected by SLR and the classification results . . . . .	48
3.3.4	Features selected by SVM-RFE and the classification results . . . . .	51
3.4	The most relevant feature set . . . . .	54
<b>4</b>	<b>Clustering analysis for mass spectrum quality assessment</b>	<b>55</b>
4.1	Introduction . . . . .	55
4.2	Clustering analysis . . . . .	56
4.2.1	Background . . . . .	56
4.2.2	Model based clustering for quality assessment . . . . .	57
4.3	Results and discussion . . . . .	61
4.3.1	The clustering results of the EM algorithm . . . . .	61
4.3.2	The salient features for EM algorithm . . . . .	61
4.3.3	Determine the quality of spectra in each cluster . . . . .	65
<b>5</b>	<b>Conclusions and future work</b>	<b>66</b>
5.1	Conclusions . . . . .	66
5.2	Future work . . . . .	67
	<b>References</b>	<b>80</b>



# LIST OF TABLES

2.1	The parameters of Mascot search engine . . . . .	21
2.2	The overall results of the denoising algorithm . . . . .	22
2.3	The distributions of the false positives and true positives in <i>ISB</i> spectra identified by the Mascot search engine . . . . .	24
2.4	The influence of charge states to the filtering results . . . . .	28
3.1	The sources of the 69 constructed features . . . . .	37
3.2	The selected features by the <i>SLR</i> model and the meanings of the selected features . . . . .	50
3.3	Compare the overall classification results using different features selected by the <i>SLR</i> model . . . . .	50
3.4	The relative importance of the 15 most relevant features ranked using a nonlinear <i>SVM-RFE</i> . . . . .	52
3.5	Compare the overall classification results using different number of features selected by the <i>SVM-RFE</i> algorithm . . . . .	53
3.6	Compare the relevance of the two feature sets selected by the <i>SLR</i> model and the <i>SVM-RFE</i> algorithm . . . . .	54
4.1	The clustering results of the <i>EM</i> algorithm . . . . .	62
4.2	The distribution of spectra in different clusters with the threshold of zero . . . . .	62
4.3	The clustering centers of the <i>EM</i> algorithm . . . . .	63
4.4	The clustering results of the <i>EM</i> algorithm using the six salient features . . . . .	65

# LIST OF FIGURES

1.1	The fragment pattern of the peptide <i>GPNAF</i> (a) and a artificial spectrum of this peptide (b) . . . . .	3
1.2	The workflow of pre-processing tandem mass spectra . . . . .	8
2.1	An example of morphological reconstruction filter . . . . .	18
2.2	Venn diagram showing the overlap between the identified spectra from the raw spectra and the denoised spectra . . . . .	23
2.3	The number of spectra whose Mascot ion scores are larger than a given value . . . . .	25
3.1	The workflow of feature selection and its verification . . . . .	35
3.2	(a) The feature selection frequency and (b) the absolute values of mean weights in the twenty-five runs . . . . .	49
4.1	Plot of the absolute values of clustering center difference in descending order . . . . .	64
5.1	The new workflow for pre-processing tandem mass spectra . . . . .	68

# LIST OF ABBREVIATIONS

<i>SVM</i>	Support vector machine
<i>SVM-RFE</i>	Recursive feature elimination based on support vector machine
<i>OSH</i>	Optimal separating hyperplane
<i>LR</i>	Logistic regression
<i>SLR</i>	Sparse logistic regression
<i>EM</i>	Expectation maximization
<i>LDA</i>	Linear discriminative analysis
<i>FLDA</i>	Fisher linear discriminative analysis
<i>MS/MS</i>	Tandem mass spectrometry
<i>Th</i>	Thompson, the unit of mass-to-charge ratio
<i>TIC</i>	Total ion current
<i>TPR</i>	True positive rate
<i>TNR</i>	True negative rate
<i>FNR</i>	False negative rate
<i>ROC</i>	Receiver operating characteristic
<i>AUC</i>	Area under the receiver operating characteristic curve

# CHAPTER 1

## INTRODUCTION AND PROBLEM DESCRIPTION

### 1.1 Background

Proteins are the primary components of living cells and accomplish most functions of living cells [Hun93]. For example, some proteins define the shape and form of cells. Other proteins may identify foreign substances and create an immune response, turn genes on and off, function as enzymes to control chemical reactions in cells, or transport oxygen, nutrients and wastes into and around cells etc. In molecular biology, understanding the functions of proteins is the foundations of explanation. The functions of proteins can be analyzed through their structures.

Proteins are long chain of amino acids. Each amino acid shares a basic structure: a central carbon atom, an amino group ( $NH_2$ ), a carboxyl group ( $COOH$ ), and a side chain group ( $R$ ). Different side chain groups define different amino acids. Generally, all proteins are composed of the twenty standard amino acids. The amino acid sequence of a protein is called its primary structure. The complex three-dimensional structure of a protein controls its basic function. Protein sequencing, which aims to determine the primary structures of proteins, is very important to determine the three-dimensional structure of proteins.

In addition to analyzing the functions of proteins, protein sequencing is very important to diagnose and treat diseases because doctors may need to analyze the proteome - the whole proteins in a tissue at once. Therefore, the large scale sequencing of the whole proteins in a tissue is essential for us to find the biomarkers that signal a disease, to find the targets for a drug and to find the medicines which suit a specific person.

In practice, proteins can be thought of being composed of small multi-amino acid subunits called peptides [KS00]. Therefore, for protein sequencing, we can sequence several peptides of a protein. Then its whole sequence can be inferred. So peptide sequencing is a key step in protein sequencing, and a central problem in proteomics research, which is the large-scale analysis of proteins [AM03].

Nowadays, tandem mass spectrometry (*MS/MS*) is the method of choice for peptide sequencing [NVA07]. After a protein is digested into peptides by proteases like trypsin, a tandem mass spectrometer can measure the mass-to-charge ratio ( $m/z$ ) of a peptide ion, fragment the peptide ion, and measure the  $m/z$  of the fragment ions and the intensities of these ions. Assume a peptide  $P = a_1 \dots a_n$  consists of  $n$  amino acids, where  $a_i, i = 1, \dots, n$  is one of the twenty amino acids. The mass of the peptide is calculated by

$$m(P) = m(H) + m(OH) + \sum_1^n m(a_i).$$

where  $m(H)$  and  $m(OH)$  are the additional masses of the peptide's *N*- and *C*-terminals, respectively. The *N*-terminal of a peptide refers to the end of the peptide terminated by an amino acid with a free amine group ( $-NH_2$ ). The *C*-terminal of a peptide refers to the end of the peptide terminated by an amino acid with a free carboxyl group ( $-COOH$ ). A mass spectrometer typically breaks a peptide  $a_1 \dots a_n$  at different peptide bonds and detects the  $m/z$  values of the resulting partial *N*-terminal and *C*-terminal fragment ions. For example, the peptide *GPFNA* may be broken into the *N*-terminal ions *G*, *GP*, *GPF*, *GPFN* (*b*-type ions), and *C*-terminal ions *PFNA*, *FNA*, *NA*, *A* (*y*-type ions) [JP04]. Figure 1.1(a) shows its fragmentation pattern. Moreover, both the *N*-terminal and *C*-terminal ions can lose some small parts, e.g., the *N*-terminal ions may lose a *CO* group while the *C*-terminal ions may lose an *NH* group. In addition, each ion may have different charge states. A tandem mass spectrometer will measure both the  $m/z$  ratio of each ion, and its intensity, which reflects the abundance of the ion of a given  $m/z$  detected in the mass spectrometer. Thus each tandem mass spectrum produced by a tandem mass spectrometer is composed of many peaks (fragment ions), and each peak is

represented by its  $m/z$  value and intensity value. Figure 1.1(b) shows an artificial spectrum of peptide *GPFNA*.

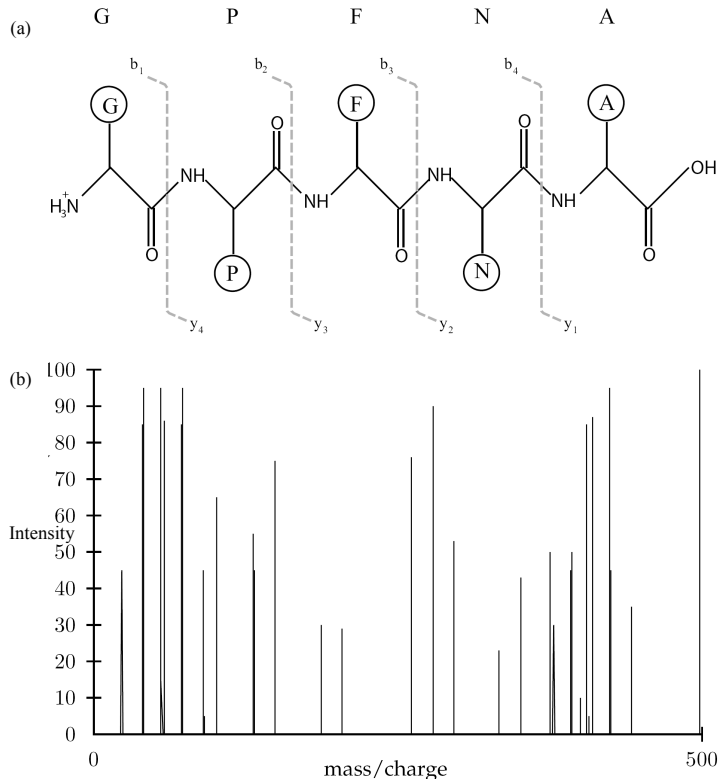


**Figure 1.1:** The fragment pattern of the peptide *GPFNA* (a) and a artificial spectrum of this peptide (b) [JP04]

Two approaches are widely used for peptide identification from tandem mass (MS/MS) spectra: database searching [BE01, ZAS02, SYI03, LTK+04, NTV+05, FA05, ZSZ+06, WYC06, WTE07, LBB+07, KHG08] and *de-novo* sequencing [DAC+99, HZM00, MZH+03, BTBP04, FP05, FRR+05, MZL05, GRC+05, BCG07]. *De-novo* sequencing algorithms assign peptides to *MS/MS* spectra based on the spectra alone. Therefore these algorithms are invaluable for the identification of both known and unknown peptides. However, *de-novo* algorithms are most useful when spectra have complete (all the *b*- ions or *y*- ions of a spectrum are present) or nearly complete fragment peaks and less noisy peaks, because they rely on the presence of successive *b*- or *y*- ions to find a whole peptide sequence or a sequence tag. *De-novo* algorithms may find ambiguous sequences for real-world spectra because many spectra are far from complete. On the other hand, if a database of all proteins from a

genome is accessible, peptides can be assigned to spectra by searching the peptides in the database [JP04]. Database search based algorithms are currently the leading peptide identification methods. Most database search approaches employ a score function. Different search engines such as Sequest [EMY94] and Mascot [PPDC99] adopt different scoring systems. Experiments show that using multiple search engines may yield better results [KSC<sup>+</sup>05]. Therefore, some researchers have combined the results of different search engines to assign peptides to spectra. For example, the program Scaffold [EHFG05] assigns probabilities to the search results from different peptide identification algorithms such as Mascot [PPDC99], Sequest [EMY94], X!Tandem [CB04], Phenyx [CMG<sup>+</sup>03], Spectrum Mill (Agilent Technologies), and OMSSA [GMK<sup>+</sup>04]. By using the above strategy, it is expected to improve the performance of peptide identification from *MS/MS* spectra. However, with the steady increase of the database size, more and more peptides similar to the one investigated can be present in the searched database. On the other hand, the spectrum may contain very few signal peaks or weak signal peaks whose intensities are indistinguishable from those of noise peaks [GKPW03]. Spectral pre-processing, becomes very important in today's proteomics research to improve the reliability of assigning peptides to spectra.

Tandem mass spectrum pre-processing aims at processing spectra produced by tandem mass spectrometers to increase both the accuracy and efficiency of subsequent peptide identification from spectra [HKPM06, NVA07]. Five types of pre-processing methods are widely used: spectrum normalization [BGMY04, NP06, DSZW08], spectrum clustering [FBS<sup>+</sup>08, FMH<sup>+</sup>07], precursor charge determination [SED<sup>+</sup>02, KWMN05, TSS<sup>+</sup>06, SHH08, NPL08, ZDSW08], spectrum denoising [BCG<sup>+</sup>02, RCA<sup>+</sup>04, KL07, ZHL<sup>+</sup>08, DSPW09], and spectrum quality assessment [PKK04, BGMY04, NRG<sup>+</sup>06, FMV<sup>+</sup>06, SMF<sup>+</sup>06, CT07, WGDP08, WDP08, ZWDP09]. It is believed that these pre-processing algorithms can increase the number of identified peptides and improve the reliability of peptide identification from tandem mass spectra. Now, spectral pre-processing has become a critical module in many high throughput data processing pipelines. Both database search and *de-novo*

peptide identification algorithms can benefit from these pre-processing methods. Because these pre-processing algorithms increase the number of identified peptide, and save much time for peptide identification from tandem mass spectra, they are particularly useful for the design of real-time control methodologies for tandem mass spectrometers.

Nowadays, to improve the throughput and efficiency of mass spectrometry, researchers try to design real-time control methodologies for mass spectrometers. Here the timing is critical because we want to identify peptides and proteins in the process of a tandem mass spectrometry experiment in a very short time period. One of the key modules of the methodologies is spectral quality assessment which tries to objectively determine the quality of spectra, and the poor quality spectra which are not interpretable by peptide identification algorithms are removed from further analysis. Because only high quality spectra are further analyzed by peptide identification algorithms, we can save the time wasted in searching the poor quality spectra. However, other pre-processing schemes are also important for the design of these real-time control methodologies. For example, denoising methods remove most noisy peaks. Thus the denoised spectra have far fewer noisy peaks than the undenoised spectra, and the process of assigning peptides to spectra can be accelerated by using the denoised spectra instead of the original spectra. On the other hand, the signal-to-noise ratios of spectra are increased because most noisy peaks are removed. The reliability of assigning peptides to spectra is also improved.

## 1.2 Objectives

Pre-processing tandem mass spectra is a very important module for developing real-time control methods of tandem mass spectrometers. The objective of this research is to develop methods for pre-processing tandem mass spectra. Specifically in this thesis we will present:

- (1) A novel denoising method to filter out the noise in the tandem mass spectra and thus to improve their quality.



- (2) Feature selection methods to select the most relevant features for describing the quality of tandem mass spectra.
- (3) Quality assessment methods to classify tandem mass spectra into high quality and poor quality.

### 1.3 Spectral pre-processing

Generally, spectral pre-processing methods can be divided into low level and high level methods [HMA06]. The low level methods transform the continuous spectral data (raw data) from mass spectrometers into list of peaks. These low level methods may include peak centroiding, noise filtering, calibration, deisotoping, and deconvolution. However, most raw data are processed directly by instruments' software. In this study we concentrate on high level pre-processing methods which are often performed on the peak lists. Widely used high level pre-processing methods include spectral clustering, precursor ion charge determination, spectral intensity normalization, denoising, and automatic quality assessment of tandem mass spectra.

Spectral clustering algorithms detect spectra that are produced by the same peptide and replace them with only one representative spectrum [FBS+08, TMW+03]. In tandem mass spectrometry experiments, some spectra are generated from the same peptide. When spectra are collected from a number of runs, the spectra from one peptide may be recorded thousands of times. After clustering analysis, we can use a single representative spectrum to represent all spectra produced by the same peptide. Analyzing only representative spectra results in significant speedup of *MS/MS* database searches.

Automatic charge state determination of precursor ions can save a lot of time of peptide identification algorithms. For most database search based peptide identification algorithms, when the accurate charge state of the precursor ion of a spectrum is not known, the spectrum is searched multiple times assuming different charge states. This blind strategy double or multiple the search time of peptide identification algorithms. Nowadays, many algorithms try to determine the charge state

of the precursor ions [CMD<sup>+</sup>03, KW MN05, NPL08, TSS<sup>+</sup>06, ZDSW08]. For high resolution spectra, digital signal processing based methods are widely used to predict the charge states of precursor ions; for low resolution spectra, machine learning based algorithms are good choices.

This thesis focus on denoising tandem mass spectra, feature construction and feature selection, and quality assessment of tandem mass spectra. The whole workflow is given in Figure 1.2. For a typical tandem mass spectrum, about 80% of peaks are noisy peaks [KL07]. Therefore, denoising algorithms are needed to remove these noisy peaks. In addition, about 85% of spectra produced by spectrometers are poor quality spectra which can't be identified by peptide identification algorithms [WGDP08]. So quality assessment algorithms are needed to remove these poor quality spectra before peptide identification. For quality assessment, we should construct the relevant features which can discriminate high quality spectra from poor quality ones. Therefore, in this thesis we design feature selection algorithms to select those most relevant features out of the constructed features found in the literature. The intensities of tandem mass spectra are normalized because some of these features use the intensity information of peaks. Note that for the spectra from the same type of tandem mass spectrometers, these spectra share some properties. Therefore, some features may represent the quality of this type of spectra, and for this reason, one may find a small number of highly relevant features for this type of tandem mass spectra. In other words, the feature selection module can be used only once for each type of tandem mass spectrometers. After pre-processing, we can both speedup and improve the reliability of assigning peptides to spectra.

## 1.4 Overview of the rest of this thesis

In Chapter 2, we discuss denoising tandem mass spectra [DSPW09]. The novel contribution is that we design a spectral denoising algorithm to remove most noisy peaks among a spectrum. The function of a denoising algorithm is threefold. Firstly, the reliability of assigning peptides to spectra is improved as most noisy peaks are

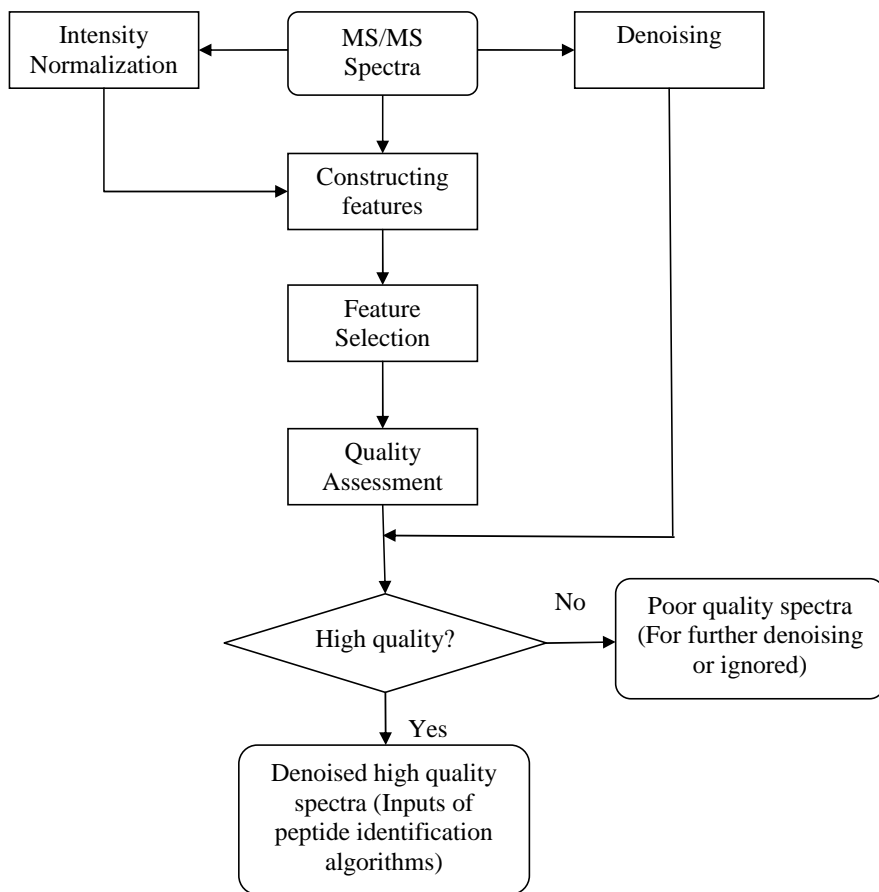


**Figure 1.2:** The workflow of pre-processing tandem mass spectra

removed. Secondly, the efficiency of assigning spectra to peptides is also improved as there are far less peaks in a spectrum after applying the denoising algorithm. Thirdly, the space for storing spectra is also decreased since the majority of noisy peaks are removed.

In Chapter 3, we address the question of how to find the features which can discriminate poor quality spectra from the high quality ones [DSZW08, DW09a, ZWDP09]. We design a two-stage recursive feature elimination procedure based on support vector machines (*SVM-RFE*) to select the most relevant features. We also design a sparse logistic regression model to select the relevant features. The importance of feature selection is twofold. Firstly, classifiers can be trained to predict the quality of spectra with high accuracy using the selected features. Secondly, we can save the time wasted in constructing the nearly irrelevant features by only constructing the relevant features.

In Chapter 4, we discuss cluster analysis for quality assessment of tandem mass spectra [DW09b, DSW09, WDP08]. We use the model based clustering technique for the quality assessment of tandem mass spectra. After removing the poor quality spectra, much time can be saved for peptide identification algorithms by not searching the poor quality spectra. In addition, the number of false positives is also decreased since most poor quality spectra are removed.

In Chapter 5, we conclude this thesis and give some directions for further improvement.

# CHAPTER 2

## DENOISING TANDEM MASS SPECTRA

### 2.1 Introduction

Tandem mass spectrometers are powerful tools for the analysis of biological complexes. In a typical tandem mass spectrometry experiment, proteins are first extracted from a biological complex. Then after a protein is digested into peptides by proteases like trypsin, a tandem mass spectrometer measures the intensities of peptide ions and fragment ions versus their mass to charge ratio ( $m/z$ ) which are called mass spectra. Tandem mass spectrometry is a complex method, and well-trained experts are needed to analyze the produced spectra [Cha]. Tandem mass spectrometry is also a high-throughput analytical method, and it can produce a large number of tandem mass spectra. In a typical tandem mass spectrum, up to 80% peaks are noise [KL07]. These noisy peaks may be derived from chemical, electrical or other sources. Therefore, it is beneficial to apply a spectrum denoising method before assigning peptides to spectra. By removing most noisy peaks, the reliability of assigning peptides to spectra can be improved. In addition, since most noise peaks are removed, the speed of assigning peptides to spectra may also be increased.

Spectrum denoising methods intend to keep signal peaks (reflecting peptide fragment ions) while removing noisy peaks (not reflecting peptide fragment ions). In fact, most peptide identification algorithms adopt denoising methods as a pre-processing step. For example, PEAKS [MZL05], PepNovo [FP05] and AUDENS [GRC+05] all have their own denoising models. However, there are many ad hoc problems for spectrum denoising issues. Firstly, the property of un-equally spaced  $m/z$  values of spectra makes it improper to directly use any standard denoising algorithms for tra-

ditional signal processing [MRH<sup>+</sup>06]. Secondly, the noise in a spectrum are hardly modeled by a single statistical model. For example, most noisy peaks are in the middle of  $m/z$  range of a spectrum, and accordingly, far fewer noisy peaks are in the two ends of a spectrum [KL07]. Besides, the peaks in the middle of  $m/z$  range tend to have higher intensities than those at the two ends.

Generally, there exist three types of spectrum denoising algorithms: threshold, digital signal processing, and machine learning or heuristic search algorithms. Threshold methods simply discard peaks with intensities below a threshold. However, the thresholds are hard to determine because a global optimal threshold may not exist for an algorithm to work well. Moreover, these methods only use the intensity information of each peak to determine whether a peak is a fragment ion or a noisy peak. These methods implicitly assume the independence of peaks without considering the interrelationship. In fact, a true fragment ion may be related to other fragment ions in a true tandem mass spectrum. For example, the mass difference of two signal ions may be equal to the mass of one of the 20 amino acids, e.g.,  $b_i, b_{i+1}$  ions.

The second type of methods uses digital signal processing procedures such as Fourier analysis and wavelet analysis for denoising spectra [RCA<sup>+</sup>04, MRH<sup>+</sup>06]. Digital signal processing methods are successfully used in other fields such as speech recognition, image processing, and computer vision. However, these methods assume that the  $m/z$  difference between peaks is a constant (interpolation is used to produce equally spaced  $m/z$  values at the expense of introducing extra peaks). Indeed, as the noise is  $m/z$  dependent, short time Fourier transform or wavelet transform are better choices than Fourier transform [Mal99]. These methods reduce the intensities of the “noisy” peaks without removing them. As with threshold methods, digital signal processing methods use the intensity information only.

The third type of methods is based on machine learning, or some heuristic search using not only intensity information of peaks but also some additional information contained in a spectrum, such as isotopic ions or complementary ions [BCG<sup>+</sup>02, ZHL<sup>+</sup>08]. However, noise are neither equally distributed in the whole

$m/z$  range of a spectrum, nor equally distributed among features extracted from a spectrum used for machine learning. As a result, the noise may degenerate the performance of classifiers, and this type of method may not perform as well as expected. Therefore, we need novel denoising algorithms which are more robust than threshold methods, do not need to introduce extra pseudo peaks, and are “adaptive” to the  $m/z$  dependence properties of noise in a spectrum.

In this chapter, we present a spectral denoising algorithm which partially solves the above mentioned shortcomings of previous denoising algorithms. The proposed algorithm first adjusts the intensities of the peaks of a spectrum using several features extracted. Then the algorithm removes the fragment ions whose intensities are not the local maxima of the intensity-adjusted spectrum using a morphological reconstruction filter [Vin93]. Experiments are conducted on two ion trap mass spectral datasets, and the results show that our algorithm can remove about 69% of the peaks which are likely noisy peaks among a spectrum. At the same time, the number of spectra that can be identified by Mascot increases by 31.23% and 14.12% for the spectra from two datasets.

## 2.2 Methods

In this study, a spectrum  $S$  with  $N$  peaks is represented by the peak list, i.e.,

$$S = \{(x_k, i_k) \mid x_k \in R^+, i_k \in R^+, 1 \leq k \leq N\}$$

where  $(x_k, i_k)$  denotes peak  $k$  with  $m/z$  value of  $x_k$  and intensity of  $i_k$ .

The proposed spectral denoising method consists of two unique modules: peak intensity adjustment and intensity local maximum extraction. The first module is used to adjust the intensities of signal peaks in a spectrum. After adjustment, intensities of signal peaks are expected to be the local maxima in a spectrum. The second module is used to select these local maxima of the signal peak intensity-adjusted spectra, and thus peaks whose intensities are not the local maxima are removed.

### 2.2.1 Peak intensity adjustment

The intensity is an important attribute of a peak in a spectrum. The empirical approaches usually assume that peaks with high intensities are more likely to be signal peaks than those with low intensities. However, there are many exceptions to these approaches. Thus to distinguish signal peaks from noisy peaks, more attributes of peaks should be taken into consideration. For example, signal peaks may have complementary peaks whose masses are added to the signal peaks to give the mass of a precursor ion.

Five features are constructed for each peak on the basis of the properties of theoretical peptide mass spectra [WGD<sup>P</sup>08]. A score for each peak is calculated by a linear combination of these features. To define these features, as in [WGD<sup>P</sup>08], four variables are introduced

$$dif1(x, y) = x - y$$

$$dif2(x, y) = x - (y + 1)/2$$

$$sum1(x, y) = x + y$$

$$sum2(x, y) = x + (y + 1)/2$$

For a peak  $(x, i)$  (for simplicity, this peak is called peak  $x$ ) of a spectrum  $S$ , the first feature  $F_1$  collects the number of peaks whose mass differences with  $x$  approximately equal the mass of one of the twenty amino acids.

$$F_1(x) = |\{y \mid \begin{aligned} &abs(dif1(x, y)) \approx M_i \text{ or} \\ &abs(dif1(x, y)) \approx M_i/2 \text{ or} \\ &abs(dif2(x, y)) \approx M_i/2 \text{ or} \\ &abs(dif2(y, x)) \approx M_i/2 \} | \end{aligned}$$

where  $|\bullet|$  is the cardinality of a set;  $abs$  is the absolute value function; and  $M_i (i = 1, 2, \dots, 20)$  is the mass of one of the twenty amino acids. In this study we consider all Methionine amino acids to be sulfoxidized and do not distinguish three pairs of amino



acids by their masses: isoleucine vs. leucine, glutamine vs. lysine, and sulfoxidized methionine vs. phenylalanine as the masses of each pair are very close. If both peaks  $x$  and  $y$  are singly charged, their difference equals the mass of one of the 20 amino acids, and  $abs(dif1(x, y)) \approx M_i$ ; if both  $x$  and  $y$  are doubly charged, their difference equals half of the mass of one of the 20 amino acid, and  $abs(dif1(x, y)) \approx M_i/2$ ; if  $x$  is singly charged while  $y$  is doubly charged,  $abs(dif2(x, y))$  equals half of one of the mass of the 20 amino acids; and if  $x$  is doubly charged while  $y$  is singly charged,  $abs(dif2(y, x))$  equals half of the mass of one of the 20 amino acids. The comparison implied by  $\approx$  uses a tolerance. Bern *et al* used  $\pm 0.37$  [BGMY04] for constructing features for the quality assessment of ion trap tandem mass spectra. Wong *et al* used  $\pm 0.3$  for fragment ion mass tolerance, and  $\pm 1$  for precursor ion mass tolerance for ion trap tandem mass spectra [WSCC07]. In this study, we use  $\pm 0.8$  for fragment ion mass tolerance, and  $\pm 2$  for precursor ion mass tolerance because these parameters seem to be reasonable for ion trap spectra for the Mascot search engine to give good peptide identification results.

The second feature  $F_2$  collects the number of peaks whose masses added to  $x$  approximately equal the mass of the precursor ion.

$$F_2(x) = |\{y \mid \begin{aligned} &sum1(x, y) \approx M_{parent} + 2 * M_H \text{ or} \\ &sum1(x, y) \approx M_{parent}/2 + 2 * M_H \text{ or} \\ &sum2(x, y) \approx M_{parent}/2 + 2 * M_H \text{ or} \\ &sum2(y, x) \approx M_{parent}/2 + 2 * M_H \} | \end{aligned}$$

where  $M_{parent}$  is the mass of the precursor ion (parent), and  $M_H$  is the mass of a hydrogen atom. As for  $F_1$ , if both peaks  $x$  and  $y$  are singly charged,  $sum1(x, y) \approx M_{parent} + 2 * M_H$ ; if both  $x$  and  $y$  are doubly charged,  $sum1(x, y) \approx M_{parent}/2 + 2 * M_H$ ; if  $x$  is singly charged while  $y$  is doubly charged,  $sum2(x, y) \approx M_{parent}/2 + 2 * M_H$ ; and if  $x$  is doubly charged while  $y$  is singly charged,  $sum2(y, x) \approx M_{parent}/2 + 2 * M_H$ .

The third feature  $F_3$  collects the number of peaks which are produced by losing

a water or an ammonia molecule from  $x$ .

$$F_3(x) = |\{y \mid dif1(x, y) \approx M_{water} \text{ or } M_{ammonia} \text{ or} \\ dif1(x, y) \approx M_{water}/2 \text{ or } M_{ammonia}/2 \text{ or} \\ dif2(x, y) \approx M_{water}/2 \text{ or } M_{ammonia}/2 \text{ or} \\ -dif2(y, x) \approx M_{water}/2 \text{ or } M_{ammonia}/2\}|$$

where  $M_{water}$  is the mass of a water molecule and  $M_{ammonia}$  is the mass of an ammonia molecule. Because  $x$  loses a molecule to form  $y$ ,  $x$  should be larger than  $y$  if they have the same charge state. Therefore, as opposed to  $F_1$ , the *abs* function should not be used here. If both peaks  $x$  and  $y$  are singly charged,  $dif1(x, y) \approx M_{water}$  or  $M_{ammonia}$ ; if both  $x$  and  $y$  are doubly charged,  $dif1(x, y) \approx M_{water}/2$  or  $M_{ammonia}/2$ ; if  $x$  is singly charged while  $y$  is doubly charged,  $dif2(x, y) \approx M_{water}/2$  or  $M_{ammonia}/2$ ; and if  $x$  is doubly charged while  $y$  is singly charged, a minus sign should be added to  $dif2(y, x)$  and  $-dif2(y, x) \approx M_{water}/2$  or  $M_{ammonia}/2$ .

The fourth feature collects the number of peaks which are produced by losing a  $CO$  group or an  $NH$  group from  $x$ .

$$F_4(x) = |\{y \mid dif1(x, y) \approx M_{CO} \text{ or } M_{NH} \text{ or} \\ dif1(x, y) \approx M_{CO}/2 \text{ or } M_{NH}/2 \text{ or} \\ dif2(x, y) \approx M_{CO}/2 \text{ or } M_{NH}/2 \text{ or} \\ -dif2(y, x) \approx M_{CO}/2 \text{ or } M_{NH}/2\}|$$

where  $M_{CO}$  and  $M_{NH}$  are the mass of a  $CO$  group and an  $NH$  group, respectively. For the same reason as for  $F_3$ ,  $x$  should be larger than  $y$  if they have the same charge state. Therefore, if both peaks  $x$  and  $y$  are singly charged,  $dif1(x, y) \approx M_{CO}$  or  $M_{NH}$ ; if both  $x$  and  $y$  are doubly charged,  $dif1(x, y) \approx M_{CO}/2$  or  $M_{NH}/2$ ; if  $x$  is singly charged while  $y$  is doubly charged,  $dif2(x, y) \approx M_{CO}/2$  or  $M_{NH}/2$ ; and if  $x$  is doubly charged while  $y$  is singly charged, the two peaks should satisfy  $-dif2(y, x) \approx M_{CO}/2$  or  $M_{NH}/2$ . The fifth feature is used to collect the number of isotope peaks associated with  $x$

$$F_5(x) = |\{y \mid x \approx y - 1 \text{ or } x \approx y - 0.5\}|$$

The adjusted intensity of each peak is the original intensity of the peak multiplied by the score computed based on the five features. The final score for peak  $x$  is calculated as:

$$Score(x) = \omega_0 + \omega_1 * f_1(x) + \omega_2 * f_2(x) + \omega_3 * f_3(x) + \omega_4 * f_4(x) + \omega_5 * f_5(x)$$

where  $f_i(i = 1, \dots, 5)$  is the normalized value of each feature (normalized to have the mean of zero and the variance of one), and  $\omega_i(i = 0, \dots, 5)$  is a coefficient. This study sets the bias  $\omega_0 = 5$  to ensure only few peaks have negative score;  $\omega_1$  and  $\omega_2$  are set to 1.0; both  $\omega_3$  and  $\omega_4$  are set to 0.2; and  $\omega_5$  is set to 0.5. These values are selected according to the normalization method of the Sequest algorithm. In this algorithm, a magnitude of 50 is assigned to the  $b$ - and  $y$ - ions in a theoretical spectrum. The neutral loss of water ions, the neutral loss of ammonia ions, and  $a$ -ions are assigned a value of 10. The ions which have mass difference of  $\pm 1$  with  $b$ - and  $y$ - ions are assigned a value of 25. In this study the values are slightly different from those of the Sequest algorithm to avoid numerical problems incurred by multiplying large numbers, but the relative importance of the value of each parameter is the same as the value of the Sequest search engine. Note that the Sequest algorithm does not consider complementary ions. However, from the study of other peptide identification algorithms such as Mascot and our own study, the complement ions are very likely to be signal peaks, e.g., the presence of complementary ions is a very important feature to predict whether a spectrum is of high or poor quality [WGDP08, DSZW08]. Therefore, the weight value for feature  $F_2$  is assigned the same as that for feature  $F_1$ . The score function is similar to linear discriminative analysis ( $LDA$ ) which combines a finite number of features into a score [DHS00].

This study does not use these features to train a classifier to classify a peak as a signal peak or a noisy peak because of the peak distribution properties of tandem mass spectra. For example, the number of peaks in the middle of  $m/z$  value range of a spectrum is larger than the number of peaks in the two ends of the spectrum, and most noisy peaks are in the middle of  $m/z$  value range. Thus the features we constructed are  $m/z$  dependent. In addition, the masses of peptides are widely

scattered, and the number of peaks of spectra are quite different. These are all challenges for machine learning algorithms. Elaborate normalization methods are necessary before using these algorithms.

The intensities of signal peaks are increased while the intensities of noisy peaks are decreased after peak intensity adjustment. However, using a simple threshold is still not effective to differentiate signal peaks from noisy peaks because the scores of peaks in a spectrum tend to be larger in the middle of the  $m/z$  range than the scores of the two end peaks because most noisy peaks are in the middle of the  $m/z$  range of a spectrum. It is more reasonable to assume that the noisy peaks in a narrow  $m/z$  range are equally distributed, and that the signal peaks are mostly the local maxima of a spectrum after peak intensity adjustment. Therefore, noisy peaks can be removed by keeping only these local maxima.

### 2.2.2 Peak local maximum extraction

This study employs an algorithm called morphological reconstruction filter [Vin93] to select the local maxima of a spectrum. The inputs of a morphological reconstruction filter are a “mask” signal which is the original signal, and a “marker” signal which specifies the preserved parts in the reconstructed signal. In this study, a mask signal is a tandem mass spectrum while its marker signal is the mask signal subtracted by a very small positive number. Morphological reconstruction filter can be considered as repeated dilations of the marker signal until the contour of the dilated marker signal fits under the mask signal [Vin93, GW07, MS90]. In each dilation the value of the marker signal at every point will take the maximum value over its neighborhood. As a result, the values of the dilated marker signal are increased except the local maxima of the marker signal which will stay the same as before. The dilation operation is constrained to lie underneath the mask signal. When further dilations do not change the marker signal any more, the process stops. At this point, the dilated marker signal is exactly the same as the mask signal except the local maxima. By comparing the mask signal and the dilated marker signal, the local maxima of the mask signal can be extracted. Figure 2.1 shows an example of morphological reconstruction filter

to extract the local maxima a one dimensional signal.

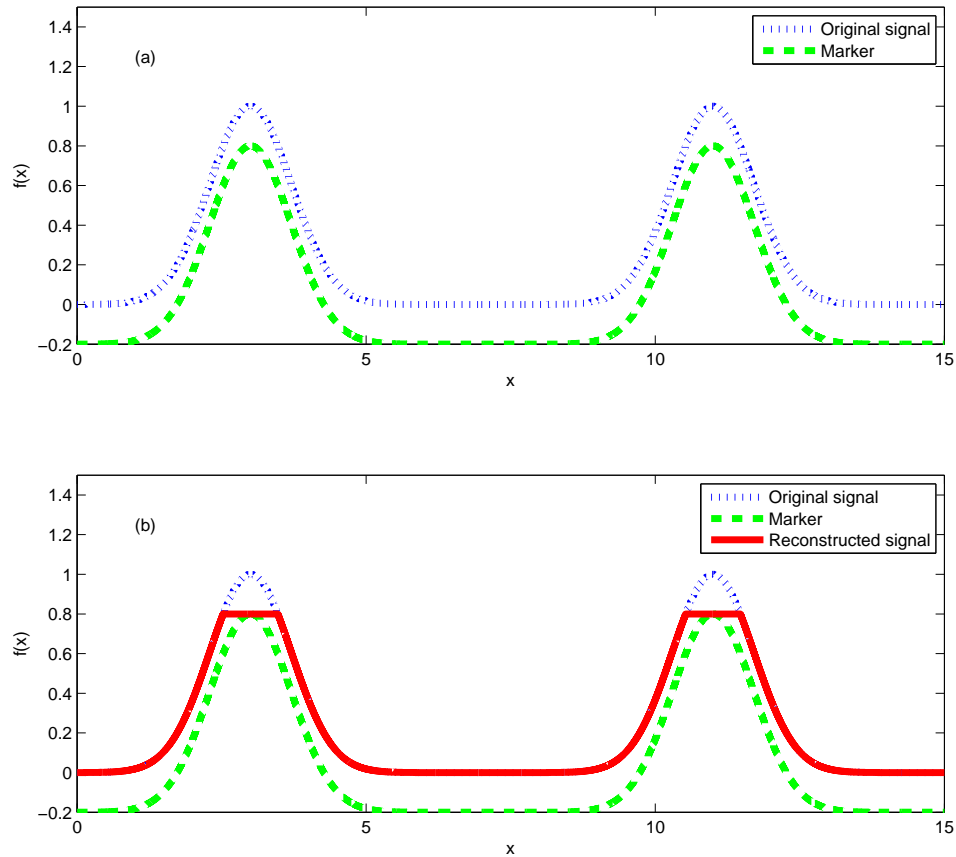


**Figure 2.1:** An example of morphological reconstruction filter. The “marker” is obtained by subtracting a small value of 0.2 from the original signal (a), and the difference between the original signal and the reconstructed signal corresponds to the local maxima of the original signal (b).

In the following, we define the morphological reconstruction filter formally. We first define the dilation operator  $\delta$  for a signal  $f(x)$

$$(\delta_B f)(x) = \max_{y \in B} f(x - y) \quad (2.1)$$

where  $B$  is called a structuring element and defined as  $B = \{-1, 0, 1\}$  here. Note that the structuring element specifies the neighborhood for conducting the morphological operations, and different structuring elements specify different neighborhoods. We

further define elementary geodesic dilation as follows:

$$\delta_g^1 f = (\delta_B f) \wedge (g) \tag{2.2}$$

where  $\wedge$  standards for the pointwise minimum. The elementary geodesic dilation operator prevents the processed signal from having larger values than the original signal. Similarly, we define the geodesic dilation of size  $n$  as applying the elementary geodesic dilation  $n$  times.

$$\delta_g^n f = \delta_g^{n-1}(\delta_g^1 f) \tag{2.3}$$

The morphological reconstruction of  $g$  from  $f$  is defined as carrying out geodesic dilation iteratively until stability is achieved.

$$\rho_g f = \bigcup_{n \geq 1} \delta_g^n f \tag{2.4}$$

Where  $f$  is the marker signal. Please see reference [Vin93] for details about the morphological reconstruction filter.

## 2.3 Results and discussion

### 2.3.1 Datasets

This study employs two ion trap tandem mass spectral datasets: *ISB* dataset and *TOV* dataset to investigate the performance of the introduced denoising algorithm. The following is a brief description of these datasets.

(1) *ISB* dataset. The spectra in *ISB* dataset are acquired from a low resolution *ESI* ion trap mass spectrometer as described in [KPN+02]. These spectra consist of 22 LC/MS/MS runs produced by Institute of System Biology (*ISB*) from 18 control mixture proteins. There are a total of 37,044 spectra in *ISB* dataset. These spectra are searched using Mascot against the ipi.HUMAN.v3.48.fasta (taken from EMBL-EBI, <http://www.ebi.ac.uk/IPI/IPIhuman.html>) containing 71,399 sequences and 5 contaminant sequences (P00760, P00761, P02769, Q29443 and Q29463

from [www.uniprot.org](http://www.uniprot.org)) appended with the sequences of the mixture proteins (from [www.uniprot.org](http://www.uniprot.org)).

(2) *TOV* dataset. The *MS/MS* spectra are acquired from a LCQ DECA XP ion trap spectrometer (ThermoElectron Corp.) as described in [WGDP06]. The number of spectra in this dataset is 22,576, and these spectra are searched using Mascot against the [ipi.HUMAN.v3.42.fasta](http://www.ebi.ac.uk/IPI/IPIhuman.html) (<http://www.ebi.ac.uk/IPI/IPIhuman.html>) containing 72,340 protein sequences and 5 contaminant sequences (P00760, P00761, P02769, Q29443 and Q29463 from [www.uniprot.org](http://www.uniprot.org)).

Similar to [MRH<sup>+</sup>06, GKPW03, ZHL<sup>+</sup>08], the Mascot search engine is used to evaluate our denoising algorithm. The raw spectra (un-denoised spectra) and the denoised spectra are searched using the Mascot search engine with the same parameters. The parameters used are given in Table 2.1. A spectrum is identified if its Mascot ion score is larger than a certain threshold. Mascot can provide two thresholds for each peptide: the homology threshold and the identity threshold [BLY<sup>+</sup>07, LBB<sup>+</sup>07, FNC07] (Note: one can find both the identity threshold and homology threshold for a spectrum by putting the cursor above the query number of the Mascot search report). Each of these two thresholds is different for different peptides. Most proteomics laboratories [BLY<sup>+</sup>07] use the identity threshold as the cut-off value to expect that the false discover rate of the peptide identification is less than (typically) 5%. In this study, we also adopt the identity threshold as the cut-off value, i.e., a spectrum is identified if its Mascot ion score is larger than its identity threshold. By doing so, the false discovery rate is expected to be less than 5% for peptide identification from both the raw and denoised spectra.

### 2.3.2 Overall spectrum denoising results

Experiments are conducted on two ion trap tandem mass spectral datasets (*ISB* and *TOV*) to illustrate the performance of the proposed spectral denoising method by comparing the Mascot search results from the raw datasets to those from the same datasets denoised by the proposed method. The results of comparisons follow as:

Table 2.2 lists the overall results of experiments. From Table 2.2, the proposed

**Table 2.1:** The parameters of Mascot search engine

---

enzyme	trypsin
fixed modifications	carbamidomethyl
variable modifications	oxidation(M)
peptide charges	+1, +2, +3
mass values	monoisotopic
protein	unrestricted
peptide mass tolerance	$\pm 2Da$
fragment mass tolerance	$\pm 0.8Da$
max.missed cleavages	1

---

denoising algorithm can remove about 68.59% ( $= (156 - 49)/156$ ) of peaks among a spectrum from *ISB* dataset, and about 68.64% ( $= (118 - 37)/118$ ) of peaks among a spectrum from *TOV* dataset. These removed peaks are possible noisy peaks because Mascot performs better after these peaks are removed as discussed below. This study also records the rough Mascot search time (in minutes). From Table 2.2, by using the proposed denoising algorithm about 13.04% ( $= (23 - 20)/23$ ) of search time is saved for the spectra of *ISB* dataset, while about 7.14% ( $= (14 - 13)/14$ ) of search time is saved for the spectra of *TOV* dataset. The results illustrate that the proposed method can reduce the time for the process of assigning peptides to spectra because most noisy peaks of a spectrum are removed, especially when the number of spectra in a dataset is large.

The number of identified peptides is increased by applying the proposed denoising method. In Table 2.2, the number of identified spectra increases by 31.23% ( $= (1458 - 1111)/1111$ ) for the spectra of the *ISB* dataset, and 14.12% ( $= (2214 - 1940)/1940$ ) for the spectra of the *TOV* dataset. The increasing rate of the newly identified spectra after applying the proposed denoising method is greater for the spectra in *ISB* dataset than for the spectra in *TOV* dataset. The first reason may be that the spectra in *ISB* dataset have more noisy peaks than those in *TOV* dataset. For example, the mean of the number of peaks for the spectra in *ISB* dataset is 156



**Table 2.2:** The overall results of the denoising algorithm. The “Raw” spectra are the original un-denoised spectra, and “Denoised” spectra are the denoised spectra. The “Mean peaks” measure the mean of the number of peaks of each spectrum in the dataset; and “Identified” is the number of spectra whose ion scores are greater or equal to the Mascot identity threshold. “Time” is the Mascot search time used in minutes.

Datasets	Mean peaks	Identified	Time (Minute)
<i>ISB</i>			
Raw	156	1111	23
Denoised	49	1458	20
<i>TOV</i>			
Raw	118	1940	14
Denoised	37	2214	13

while that is only 118 for the spectra in *TOV* dataset. The second reason may be that the “quality” of the spectra in *ISB* dataset is inferior to the quality of the spectra in *TOV* dataset. There are 37,044 spectra in *ISB* dataset, but only 1111 spectra (i.e.  $\sim 3\%$ ) can be identified before applying the proposed denoising method. On the other hand, there are 22,576 spectra in *TOV* dataset, while 1940 ( $\sim 9\%$ ) spectra can be identified before applying the denoising method by Mascot search engine. In addition, from Figure 2.2(a), up to 93.61% ( $= 1040/(1040 + 71)$ ) spectra identified in the raw spectra are also identified after applying the denoising algorithm for *ISB* dataset. Figure 2.2(b) shows up to 91.96% ( $= 1784/(1784 + 156)$ ) spectra identified in the raw spectra are also identified after applying the denoising algorithm for *TOV* dataset.

We compute the false negative rate of peptide identifications from the *ISB* dataset because these spectra are “standard” spectra, and were intensively studied by other groups [KPN<sup>+</sup>02, TSF<sup>+</sup>05]. Note that the spectra in *ISB* dataset are from 18 known proteins. Thus a spectrum is a false negative if its Mascot ion score is less than its identity threshold while the spectrum is identified from the 18 known proteins by other methods. A spectrum is a false positive if its Mascot ion score

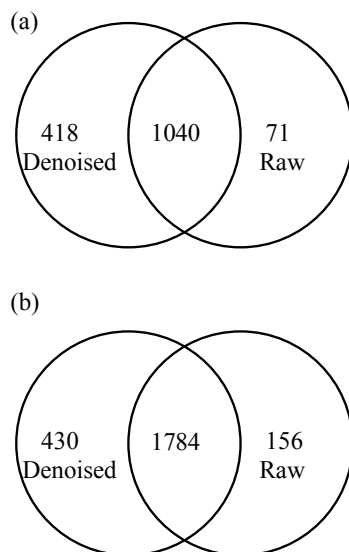


**Figure 2.2:** Venn diagram showing the overlap between the identified spectra from the raw spectra and denoised spectra of *ISB* dataset (a), and *TOV* dataset (b).

is greater than its identity threshold while the spectrum is not identified from the 18 known proteins. Combined the results from [KPN<sup>+</sup>02, TSF<sup>+</sup>05] and our manual verification, we create Table 2.3 to show distribution of the false positives, and true positives for the denoised spectra and raw spectra. From Table 2.3, 406 spectra not identified from the raw spectra are false negative for peptide identification, which results in a false negative rate of 26.96% ( $=406/1506$ ) for the raw spectral identification. Similarly, 65 spectra not identified from the denoised spectra are false negative for peptide identification, which results in a false negative rate of 4.32% ( $=65/1506$ ). In other words, the false negative rate is dramatically reduced from 26.96% to 4.32% after the proposed algorithm is applied. This indicates that Mascot can perform much better by combining with the proposed method, given the same false discovery rate of 5% controlled by the Mascot identity threshold.

### 2.3.3 The functions of each module

The proposed algorithm has two modules: intensity adjustment and peak extraction. The functions of each module in the proposed algorithm are investigated in terms of peptide ion scores. As shown in Figure 2.3, both intensity adjustment and peak

**Table 2.3:** The distributions of the false positives and true positives in *ISB* spectra identified by the Mascot search engine. The “Denoised” spectra can be identified only after denoising. The “Overlap” spectra can be identified from both the denoised and the raw spectra. The “Raw” spectra can be found only in the original un-denoised spectra. “Total” counts the sums. “False positives” are the false positives in the identified spectra, and “True positives” are the true positives in the identified spectra.

	Denoised	Overlap	Raw	Total
False positives	12	5	6	23
True positives	406	1035	65	1506
Total	418	1040	71	1529

extraction can increase the number of identified spectra, but peak extraction combined with intensity adjustment can help to identify more spectra than using either an individual module.

### 2.3.4 Discussion and further improvement

Our proposed algorithm does not need to resample each spectrum to have the same  $m/z$  distance between two adjacent peaks. Therefore, the algorithm neither introduces additional “noisy” peaks nor changes the  $m/z$  of each peak. This property is one of the advantages of our algorithm over other denoising algorithms based on Fourier analysis and wavelet analysis, e.g. MS-cleaner [MRH<sup>+</sup>06].

Unlike threshold based methods, our algorithm does not need to provide a global threshold. In fact, the morphological reconstruction filter can be considered as an adaptive signal processing method, as it “adaptively” extracts the local maxima of a spectrum. This property of morphological reconstruction filter indicates that our algorithm could be more robust than threshold based denoising algorithms [MZL05].

In the proposed algorithm, for the intensity adjustment module, the values of the parameters are chosen according to Sequest, and these values are proved to be effective in identifying peptides from spectra. For the morphological reconstruction

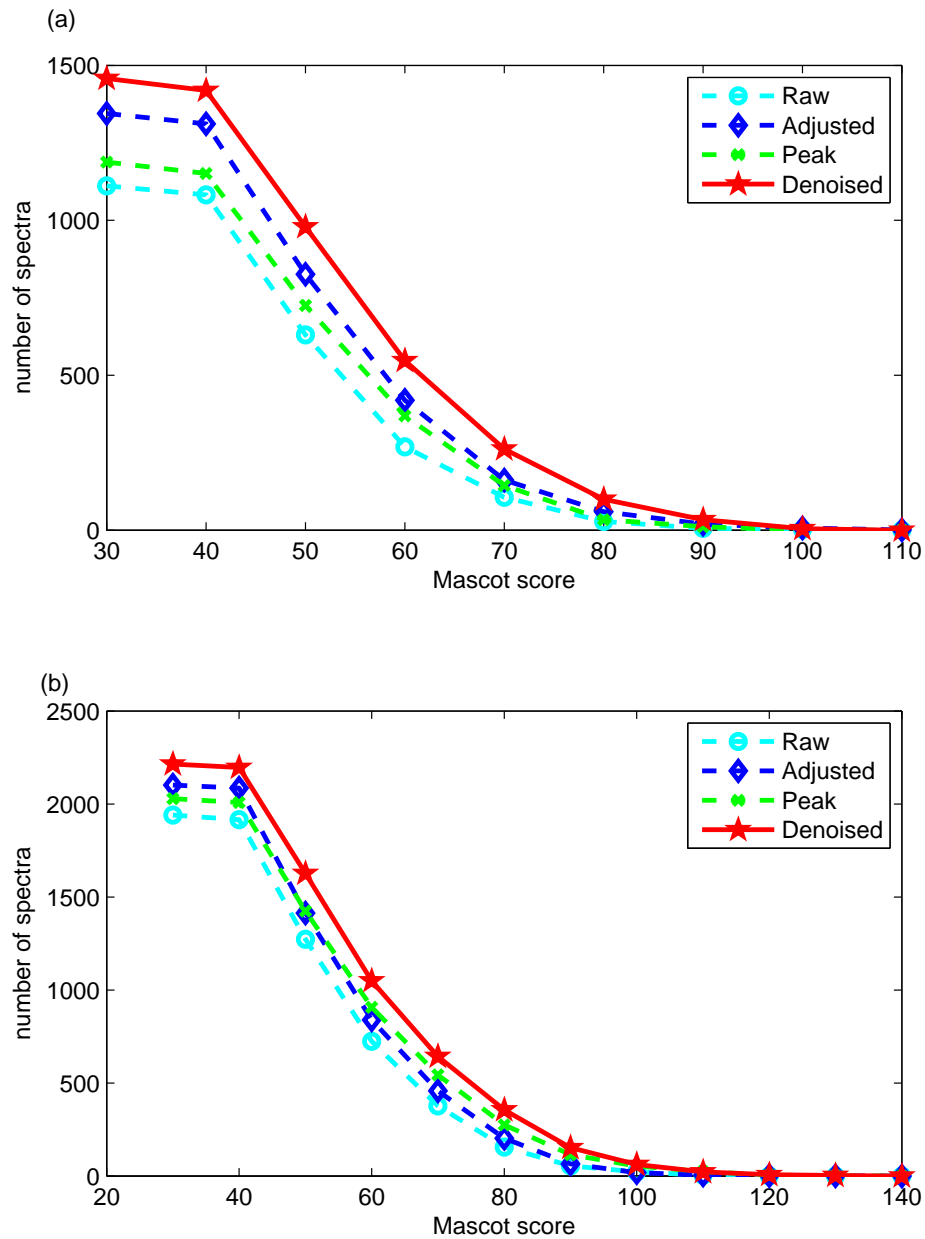


**Figure 2.3:** The number of spectra whose Mascot ion scores are larger than a given value for the raw and the processed spectra in *ISB* dataset (a) and *TOV* dataset (b). Here the “Raw” spectra are the unprocessed spectra; “Adjusted” spectra are the peak intensity adjusted spectra; “Peak” spectra are the spectra processed by the morphological filter; and “Denoised” spectra are the spectra processed by peak extraction after intensity adjustment.

filter, there is only one parameter to choose. This parameter can be set as a very small value, e.g., the smallest intensity difference between two peaks. While for the methods based on wavelet analysis, one need to choose several parameters such as the wavelet basis functions and the thresholds of the wavelet coefficients. These parameters can significantly influence the final denoising results.

The proposed algorithm uses more information about a theoretical peptide fragment ion in denoising spectra. We construct several features to adjust the intensities of a peak. Although the intensities of peaks at the two ends of each spectrum are less enhanced than those in the middle of  $m/z$  range, the intensities of signal peaks are still enhanced more than those of the noisy peaks. Thus the signal peaks are still local maxima of a spectrum, and the morphological reconstruction filter can correctly discriminate the signal peaks from noisy ones. From this point of view, our method is more robust than machine learning based denoising algorithms [ZHL<sup>+</sup>08] because our algorithm decreases the influence of the unequally distributed noise in tandem mass spectra.

The influence of the denoising method is different to the spectra with different charge states. As shown in Table 2.4, Mascot can identify another 177 triply charged spectra in *ISB* dataset after applying the proposed denoising algorithm, i.e., about 42.34% (= 177/418) of newly identified spectra are triply charged. The number of triply charged spectra accounts for about 33.80% (= 24/71) of the lost spectra. Therefore the proposed denoising method can help to find more triply charged spectra. This phenomenon is more obvious for the spectra in *TOV* dataset. For example, about 24.88% (= 107/430) of newly identified spectra are triply charged, while only 12.82% (= 20/156) of spectra are triply charged of all the lost spectra after applying the denoising algorithm. While for singly charged spectra, although the denoising method can increase the number of identified spectra, the singly charged spectra account for about 15.49% (= 11/71) of the lost spectra. This number is relatively large taking into consideration the small number of originally identified singly charged spectra. Therefore, one can expect that a denoising algorithm which employs several properties of a tandem mass spectra (such as charge state and number

of peaks [ZHL<sup>+</sup>08]) performs better than the one which employs a single property of a tandem mass spectrum.

The proposed denoising algorithm can be tuned to pre-process tandem mass spectra for other peptide identification algorithms such as Sequest or *de-novo* algorithms. Note that Sequest algorithm is based on convolution technique. The convolution results are determined by the peaks which have extra-large intensities even if experimental spectra are normalized first in Sequest algorithm. For this reason, we may need to design other spectral normalization algorithms [BGMY04, DSZW08] or change the intensities of peaks which are not removed after applying the denoising algorithm back to their original intensities. Anyway, because noisy peaks are removed, peptide identification algorithms can benefit from the proposed denoising algorithm. But for specific peptide identification algorithms, because their different use of intensity information of spectra, specific normalization algorithms are needed for these algorithms to work optimally.

A further improvement of the proposed denoising algorithm is to combine denoising algorithms with quality assessment algorithms for pre-processing tandem mass spectra. By this way, we can improve the reliability of assigning peptides to spectra, and increase the information that can be extracted from tandem mass spectra. For example, if the features used for enhancing intensities of peaks of a spectrum are very small, this spectrum may be a poor quality spectrum, and this spectrum can be excluded from further processing.

## 2.4 Conclusions

This chapter has presented a spectral denoising algorithm. The proposed algorithm first adjusts the intensities of spectra. After peak intensity adjustment, the intensities of signal peaks in a spectrum become local maxima of the spectrum. Second, the peak intensity-adjusted spectra are filtered using a morphological reconstruction filter. The signal peaks are kept while the noisy peaks are removed after applying the morphological reconstruction filter. By applying the denoising method, about 69%

**Table 2.4:** The influence of charge states to the filtering results. Here “Single”, “Double” and “Triple” represent different charge states. The “New” spectra are the newly identified spectra after denoising. The “Overlap” spectra can be identified from both the denoised and the raw spectra. The “Lost” spectra are lost after denoising.

Datasets	Single	double	triple	Total
<i>ISB</i>				
New	20	221	177	418
Overlap	12	695	333	1040
Lost	11	36	24	71
<i>TOV</i>				
New	14	309	107	430
Overlap	12	1638	134	1784
Lost	5	131	20	156

of peaks of a spectrum can be removed. At the same time, the number of spectra that can be identified by Mascot algorithm increases by 31.23% and 14.12% for the spectra in *ISB* dataset and *TOV* dataset, respectively. In summary, the proposed algorithm can remove most of noisy peaks, and increase the reliability of assigning peptides to spectra. As a result, more peptides can be identified from denoised spectra than from raw spectra.

# CHAPTER 3

## FEATURE SELECTION FOR TANDEM MASS SPECTRUM QUALITY ASSESSMENT

### 3.1 Introduction

For a typical spectrum produced by tandem mass spectrometers, about 80% of peaks are noise [KL07], most of which can be removed by denoising algorithms. In addition to the noisy peaks in spectra, many spectra are of poor quality (or called noisy spectra), e.g., the spectra produced by chemical noise. These poor spectra can't be identified by any peptide identification algorithms because they may not contain enough fragment ions. These poor quality spectra prolong the processing time of peptide identification algorithms. Moreover, they may cause false identifications because poor quality spectra may give perfect peptide matches in database search by pure chance alone [SMF<sup>+</sup>06]. Therefore, there is a great need to design automatic spectrum quality assessment algorithms, which can be used to filter out poor quality spectra before peptide identification.

Automatic spectrum quality assessment has become an important module for peptide identification from tandem mass spectrum data. Quality assessment is first used for filtering out poor quality spectra before database search [TEYI01], and is also used for post-processing of spectra after database search. For example, Nesvizhskii *et al* [NRG<sup>+</sup>06] used quality assessment to find high quality spectra which had not been annotated by a first pass database search. These high quality un-annotated spectra are important because they may be produced by new peptides which are not in the database, or because they are produced by unexpected modifications on pep-



tides. In addition, spectrum quality assessment can also be used for finding false positives after database search [FMV<sup>+</sup>06]. Because of the vast number of spectra produced in a mass spectrometry experiment, automatic quality assessment of tandem mass spectra relies on the application of computational methods.

Machine learning methods, especially supervised learning methods, are widely used for spectrum quality assessment. Such methods include preliminary rule-based methods [PKK04, TEYI01], decision tree and random forest [SMF<sup>+</sup>06], naive Bayes [FMV<sup>+</sup>06], logistic regression [WSCC07], Fisher linear discriminative analysis (*FLDA*) [WGDP08] and quadratic discriminative analysis (*QDA*) [BGMY04, XGB<sup>+</sup>05]. Recently, as the popularity of support vector machines (*SVM*) used in bioinformatics [Nob06], it is also adopted for quality assessment of tandem mass spectra [BGMY04, NP06]. Regression analysis, such as linear regression [BGMY04], which gives continuous outputs is also considered as an alternative. Recently, Wu *et al* [WDP08] prioritized unsupervised learning methods such as mean-shift for quality assessment [GSM03, CM02]. To use machine learning methods, a fixed-length vector of real value features is used to represent an original spectrum.

To design an effective automatic spectrum quality assessment algorithm, the challenging task is to find the relevant features which can best discriminate poor quality spectra from the ones containing valid peptide information. The overall accuracy of classifiers can be degraded if important information is not included in the feature vectors. On the other hand, we should avoid introducing features which have no or little power to represent the quality of a spectrum. These nearly irrelevant features may degenerate the performance of classifiers. Besides, it is time and storage wasting to gather these nearly irrelevant features. In the previous work, the features used seem to be arbitrary. Some constructed dozens or even more than one hundred features [BGMY04, FMV<sup>+</sup>06], while others constructed only two features [NP06]. Little attention has been paid to which features are most relevant to the quality of a spectrum [FMV<sup>+</sup>06, SMF<sup>+</sup>06].

In this chapter, we focus on selecting the relevant features for automatic spectrum quality assessment. We first construct most features that can be found in

the literature, and then use a sparse logistic regression (*SLR*) method and a recursive feature elimination based on support vector machines (*SVM-RFE*) [DR05, GWBV02, RGE03, TZH07] to select the most relevant features. Experiments are conducted on two datasets, and the results show the performance of classifiers based on the selected features is very promising.

## 3.2 Feature selection

### 3.2.1 Background

Feature selection in machine learning (or variable selection in statistics) aims at removing irrelevant and redundant features. The irrelevant features do not contribute to solving classification problems. The redundant features are correlated and thus can be represented by only one feature. The removing of irrelevant features and redundant features may improve classifiers' performance, decrease storage requirements and speedup algorithms, save resources in the next round of data collection and make it easier to interpret the data and visualize the data in lower dimensional space [GGNZ06, SIL07, RGE03]. Note that in many problems, feature selection does not always improve classifiers' performance. In fact, the whole feature set may be predictive since there is no information loss in them [Mur10, LM07].

Feature selection methods can be classified as unsupervised, semi-supervised and supervised methods based on whether the label information (dependent variable) is used for feature selection or not. In the past, most feature selection methods are supervised, e.g., the widely used penalized feature selection methods which minimize a loss function while imposing a penalty term to shrink some coefficients to zero [Tib96, HCM<sup>+</sup>08, MH08]. Feature selection is achieved by removing the features with zero coefficients. Unsupervised feature selection has gained attention as unlabeled data have been explored [Gue08, DB04, LM07]. A broad part of unsupervised feature selection algorithms aim at eliminating redundant features [VGLH06, MMP02]. For unsupervised feature selection methods, there is no label information guiding the

feature selection process. For this reason, some assumptions are needed to define the relevant features. For example, He *et al* [HCN05] assumes relevant features should preserve the local structure of the data. While Dash *et al* [DCSL02] assume that uniformly distributed features do not provide useful information for clustering. Clustering quality measures are also used to evaluate feature sets [LFJ04, DB04, RD06]. For semi-supervised feature selection, it is only recently used as the popularity of semi-supervised learning research [ZL07].

Feature selection methods can also be classified as univariate methods if features are ranked individually and multivariate methods if feature sets are ranked instead of individual features [HK08]. Typically, univariate methods use hypothesis testing to rank features. As a result, these methods are very fast but can't detect redundant features. Moreover, univariate methods may fail to select the features which are irrelevant individually but become relevant in the context of others [GGNZ06]. On the contrary, multivariate methods overcome the shortcoming of univariate methods by considering the dependence of features. However, as the number of feature subsets increases exponentially with the number of features. It is not practical to enumerate all the feature subsets and determine their relevance. Carefully designed methods are needed to search for the optimal feature subsets.

Feature selection has three aspects: models, search strategies and evaluation [LM98, LM07]. The three typical models are filter models, wrapper models and embedded models [LM07]. For a filter model, some criteria are applied for feature selection, i.e., features are selected by  $t$ -test or the correlation coefficients between features and the label. In contrast to filter models, the wrapper models select features by employing specific learning algorithms and optimizing the learning objective functions. For embedded models, the feature selection process is also the classifier construction process, i.e., the decision tree algorithm is a typical embedded model [Bre98]. Most filter models are univariate feature selection which ranks features individually. Such models are fast and effective, especially for the problems with high dimensionality and relatively small number of samples. In contrast to filter models, most wrapper models are multivariate methods which rank sets of features. These

models may achieve better results but may take longer time and cause overfitting problems more easily than filter models. The embedded models may be faster than wrapper models since they do not need to do cross validations and have higher capacity than filter models because most embedded models are multivariate methods.

Generally, three types of search strategies are widely used: forward selection, backward elimination and randomized feature selection [LM07, GGNZ06]. The forward selection methods start with an empty set and progressively add new features. The widely used Lasso is a type of forward selection method [Tib96]. The backward elimination methods start with a set of all possible features, and progressively remove the most irrelevant features. In contrast to forward selection and background elimination, the randomized search strategy uses randomization for feature selection. For different applications, one search strategy may be preferred over the others. The forward selection and the backward elimination algorithms may select different feature set, and the latter may be more time consuming than the former algorithm. Randomization provides an alternative search strategy, and in many situations, the randomized algorithms are either the simplest or the fastest, and even both [LM07].

There are three criteria widely used to evaluate a feature selection algorithm: the classification performance, the number of selected features and the stability of the selected feature set [LM07, GGNZ06, HK08]. One can compare the performances of classifiers trained with the whole features and the selected features. However, we should note that feature selection is not confined to improve classifiers' performance. For some applications, the number of selected features is more important than the classifiers' performance. In addition, domain experts may expect the selected feature set is stable under different experimental conditions for ease of interpreting the data [SAdP08]. To compare the performance of different feature selection algorithms, the evaluation criteria should be computed under the same experimental setting.

In feature selection, the bias produced should be avoided [LZN08, AM02]. The term "feature selection bias" has two meanings. The first one refers to the performance evaluation bias which is incurred by using the same dataset for feature selection and for testing the relevance of the selected features. Using this type of

biased testing methods, one may get perfect classification as the number of features increase even on randomly generated datasets [AM02]. The second (less noticed) feature selection bias refers to the bias incurred by removing features because the removed features may have useful information. The bias can be avoided by assuming a statistical model for the joint distribution of features and label [LZN08].

### 3.2.2 The workflow for selecting the most relevant features

Figure 3.1 shows the workflow of a feature selection method and the verification of the relevance of the selected features. Firstly, as the intensity of mass spectra is highly variant, we introduce a local cumulative normalization method to normalize spectrum intensity. The normalized intensity instead of the original intensity is used as weight when we construct some features. Secondly, to use machine learning methods for automatic spectrum quality assessment, each original spectrum is represented by a feature vector. In the feature construction step, this study collects all possible features found in the literature to represent a spectrum. Thirdly, we select the most relevant features out of the constructed features. Fourthly, to test the effectiveness of the selected features, classifiers are trained using the selected features to predict the quality of spectra. In the following, we introduce each stage of the workflow.

### 3.2.3 Local cumulative normalization

Intensity of spectra contains useful information, and can increase the accuracy of the assignment of peptides to spectra. However, there are no agreed-upon ways for using intensity information because the intensities of peaks are highly variable from spectrum to spectrum [BGMY04]. So instead of using the raw intensity of spectra, intensity is normalized in most cases before any analysis of spectra. For example, relative intensity normalization divides the raw intensity of each peak by the intensity of the most abundant peak or the total intensity of all the peaks in a spectrum. However, relative intensity normalization is sensitive to a few strong peaks in a spectrum. On the other hand, rank based intensity normalization [BGMY04] is

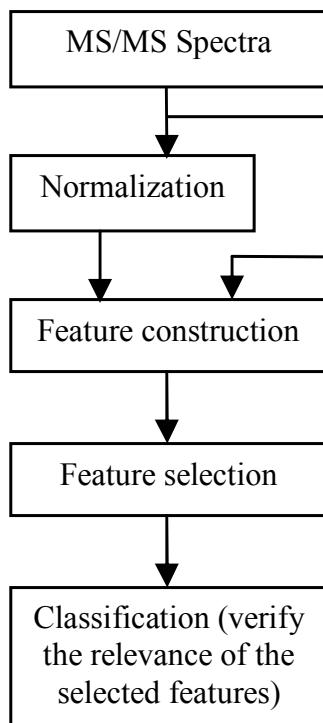


**Figure 3.1:** The workflow of feature selection and its verification used for selecting the most relevant features for quality assessment of tandem mass spectra.

very robust to intensity variation. Here “rank” means the order of a peak’s intensity magnitude in a spectrum. However, one of the drawbacks of rank based intensity normalization is that only the rank of a peak is considered without any regard to the magnitude of the peak’s raw intensity. So rank based normalization may lose useful information. Recently, a new intensity normalization method called “cumulative intensity normalization” [NP06] has been introduced. It uses both the magnitude of each individual peak and the rank of its raw intensity to normalize spectra. The cumulative normalized intensity of the  $n$ -th highest peak of a spectrum is defined as follows [NP06]:

$$I_{norm}(n) = \frac{\sum\{I_{raw}(m/z) | Rank(m/z) \geq n\}}{TIC} \quad (3.1)$$

where  $I_{norm}$  is the normalized intensity,  $I_{raw}$  is the raw intensity of a fragment ion (peak) at  $(m/z)$ ,  $TIC$  (total ion current) is the total intensity of a spectrum, and  $Rank(m/z)$  represents the order of a fragment ion at  $m/z$  when sorted by the magnitude of raw intensity in the descending order.

Although the cumulative normalization is a relatively robust method, and it can increase the number of identified peptide by the SEQUEST search engine [NP06], it is a “global” method which does not take the effects of mass-to-charge ratio on peak’s intensity into consideration. For a typical tandem mass spectrum, the peak intensity is usually higher in the intermediate  $m/z$  range, while both the high and the low  $m/z$  ranges are usually composed of peaks with lower intensities [BCG+02]. Thus, only considering the absolute abundance of peaks is not sufficient to normalize spectra. It would be better to take the difference between regions into consideration.

We introduce a “local cumulative normalization” method here. The local cumulative normalization method calculates the normalized intensity by formula (3.1) using the ranks of peaks over a window with the width of 56 thompson ( $Th$ ), instead of the global rank in [NP06].  $Th$  is the unit of  $m/z$  ratio, which is defined as

$$1Th = 1 \frac{u}{e} = 1 \frac{Da}{e}$$

where  $u$  represents the atomic mass unit;  $Da$  represents the unit *Dalton*; and  $e$  represents the elementary charge which is the electric charge unit in the atomic unit system ([http://en.wikipedia.org/wiki/Thomson\\_\(unit\)](http://en.wikipedia.org/wiki/Thomson_(unit))). The value of 56 is used because it is the maximum integer that is less than the minimum mass of the 20 amino acids. This local normalization method is expected to perform better than the global normalization method in [NP06] because local normalization un-correlates the mass-to-charge ratio and the intensity, i.e., the normalized intensity of each peak is determined by its neighbours’ intensity. So peaks at the both ends of a spectrum have a chance to have the highest intensity of one if their intensities are the local maxima of the window. This method is similar to the one used by Wong *et al* [WSCC07] except that they normalize each peak using a rank based method.

The local accumulative normalization method is used as a pre-processing step before constructing features in this study. It may also be useful for peptide identification algorithms to increase performance. Local normalized intensity is used as weight when we construct features. Using normalized intensity instead of the original intensity as weight can significantly decrease the influence of high variance of

spectral intensity which can degenerate the performance of classifiers.

### 3.2.4 Feature construction

In this study, all features that can be found in the literature are collected. At last, totally 69 features are constructed. Table 3.1 lists the sources of these features. Note that some features are exactly the same. The existence of these colinear features is problematic for a number of machine learning algorithms such as the linear regression method. In this study, each spectrum is mapped into a 69 dimensional feature vector whose components are these introduced features below.

**Table 3.1:** The sources of the 69 constructed features

Wu <i>et al</i> [WGDP08]	$W_1 \sim W_{12}^a$
Bern <i>et al</i> [BGMY04]	$B_1 \sim F_7^b$
Na <i>et al</i> [NP06]	$N_1 \sim F_2$
Salmi <i>et al</i> [SMF+06]	$S_1 \sim S_{10}^c$
Wong <i>et al</i> [WSCC07]	$\hat{W}_1 \sim \hat{W}_9$
Flikka <i>et al</i> [FMV+06]	$F_1 \sim F_{17}^d$
Purvine <i>et al</i> [PKK04]	$P_1 \sim P_3$
Xu <i>et al</i> [XGB+05]	$X_1 \sim X_5$
Nesvizhskii <i>et al</i> [NRG+06]	$\hat{N}_1 \sim \hat{N}_4^e$

<sup>a</sup> here we use normalized intensity as weight when we construct these features.

<sup>b</sup> the 7 handcrafted features.

<sup>c</sup> here the 4-th feature is deleted while the 8-th feature is separated into three features.

<sup>d</sup> the 17 manually specified features.

<sup>e</sup> the sequence tags.

Bern *et al* [BGMY04] used seven features to describe the quality of each spectrum. These features are the number of peaks ( $B_1$ ), the total ion current (*TIC*) ( $B_2$ ), the Good-Diff Fraction, which measures how likely two peaks are to differ by the mass of an amino acid ( $B_3$ ), the total intensity of peaks with isotopes ( $B_4$ ), the total intensity of peak pairs with  $m/z$  values summing to the mass of the parent ion ( $B_5$ ), the total



intensity of pairs of peaks with  $m/z$  values differing by 18 Da ( $B_6$ ), and the intensity balance ( $B_7$ ). Note that in the same paper [BGMV04], Bern *et al* use another 186 features as inputs of *SVM*, but the *SVM* does not perform well enough. Therefore, this study does not consider these 186 features.

Purvine *et al* [PKK04] proposed three features to describe the quality of each spectrum. These features are charge state ( $P_1$ ), *TIC* ( $P_2$ ), and signal-to-noise estimation ( $P_3$ ).

Xu *et al* [XGB+05] used four variables derived from five features of spectra to construct a quadratic discriminative function. The five features are the number of peaks larger than 5% of base peak intensity ( $X_1$ ), the number of peaks larger than 3% ( $X_2$ ) and 2% ( $X_3$ ) of *TIC*, the average peak distance along  $m/z$  for the peaks larger than 2% of *TIC* ( $X_4$ ) and within 1.0 ~ 1.5% of *TIC* ( $X_5$ ).

Na *et al* [NP06] used only two features to describe the quality of a spectrum. The first feature is  $x_{rea}$  ( $N_1$ ), which is computed after normalizing spectra by the cumulative normalization method [NP06]. The second feature is Good-Diff Fraction ( $N_2$ ).

Flikka *et al* [FMV+06] used 17 manually specified features, all the between-peak mass difference (deltas), and all possible  $m/z$  values to describe the quality of a spectrum. However, as stated in [FMV+06], the between-peak mass difference and all possible  $m/z$  values are not very discriminative compared to the 17 manually specified features. So we only consider the 17 manually specified features in this study. These features are the number of peaks ( $F_1$ ), the number of significant peaks ( $F_2$ ) (peaks with relative intensity greater than 0.1), the number of significant peaks divided by precursor mass ( $F_3$ ), the average delta mass in a spectrum ( $F_4$ ), the standard deviation of delta mass values ( $F_5$ ), the charge of precursor ion ( $F_6$ ), the mass of uncharged precursor ( $F_7$ ), the  $m/z$  value of a precursor in a parent spectrum ( $F_8$ ), the relative intensity of the precursor in the fragment spectrum ( $F_9$ ), the intensity difference between the top two peaks ( $F_{10}$ ), the (number of peaks)/(max\_mz - min\_mz) ( $F_{11}$ ), the number of peaks accounting for 5% of the total intensity ( $F_{12}$ ), the average of relative peak intensities ( $F_{13}$ ), the standard deviation of relative peak intensities

( $F_{14}$ ), the total raw intensities for significant peaks ( $F_{15}$ ), the total relative intensities for significant peaks ( $F_{16}$ ), the total relative intensity of complementary pairs ( $F_{17}$ ).

Salmi *et al* [SMF<sup>+</sup>06] used nine features to describe the quality of a spectrum. Some features are specific to their spectra such as the total intensity of peaks resulting from the *ICAT* reagent. Based on these nine features, for general spectra, we construct ten slightly different features. These features are: the average intensity of the peaks in the spectrum ( $S_1$ ), the standard deviation of the peak intensities in the spectrum ( $S_2$ ), the total intensity of exceptionally high peaks in the spectrum ( $S_3$ ), the presence of immonium ions in the spectrum ( $S_4$ ), the total intensity of fragment  $y_1$  ion peak ( $S_5$ ), the total intensity of the precursor peak ( $S_6$ ), the total intensity of  $y_{n-2}$  ion ( $S_7$ ), the total intensity of  $b_2$  ion ( $S_8$ ), the total intensity of  $b_{n-1}$  ion ( $S_9$ ), and a score based on mass-ladder ( $S_{10}$ ).

According to the properties of theoretical spectra and the principle of peptide fragmentation by tandem mass spectrometers, Wu *et al* [WGDP08] used twelve features to describe the quality of a spectrum. These features can be classified into four categories: the first three features ( $W_1, W_2, W_3$ ) are the number of peaks with the difference of the mass of one of the 20 amino acids, ( $W_4, W_5, W_6$ ) are the number of peaks with  $m/z$  values summing to the mass of their parent ion, ( $W_7, W_8, W_9$ ) are the total number of peaks with  $m/z$  values differing by the mass of a water molecule or an ammonia molecule, ( $W_{10}, W_{11}, W_{12}$ ) are the total number of peaks with  $m/z$  values differing by the mass of a *CO* group or an *NH* group. Here we use normalized intensity as weight when we construct these features although the intensity was ignored in [WGDP08].

Recently, seven out of nine features were used to construct a logistic regression model to predict the quality of tandem mass spectra by Wong *et al* [WSCC07]. These features are the number of peaks in a spectrum ( $\hat{W}_1$ ), normalized *TIC* ( $\hat{W}_2$ ) (because we do not know which spectra were produced by a specific run, we just use *TIC* instead), GoodSegs ( $\hat{W}_3$ ), the ratio of the number of peaks which have relative intensities greater than 1% of the total intensity to the total number of peaks in a spectrum ( $\hat{W}_4$ ), the ratio of the number of peaks that have relative intensities greater

than 20% of total intensity to the total number of peaks in a spectrum ( $\hat{W}_5$ ), pairs of peaks whose  $m/z$  values add together to give the  $m/z$  of the parent ( $\hat{W}_6$ ), the presence of isotope peaks associated with an inferred  $b$  or  $y$  ion ( $\hat{W}_7$ ), the presence of water loss peaks associated with an inferred  $b$  or  $y$  ion ( $\hat{W}_8$ ), the ninth feature ( $\hat{W}_9$ ) which quantifies evidence for inferred  $b$  or  $y$  pairs separated by amino acid masses.

Nesvizhskii *et al* constructed 40 features to describe the quality of a spectrum. However, most features are considered in the previous papers. We only construct four features which are not considered by the previous papers. These features are the length of the longest sequence tag that can be extracted from a spectrum ( $\hat{N}_1$ ), the average length of all extracted sequence tags ( $\hat{N}_2$ ), the number of sequence tag of length one ( $\hat{N}_3$ ) and a derived version of  $\hat{N}_3$  computed using the peak intensities as weight factors ( $\hat{N}_4$ ).

At this point, we have introduced 69 features found in the literature to describe the quality of a spectrum. In this study, each spectrum is mapped into a 69 dimensional feature vector whose components are these introduced features. As discussed earlier, some of these features may be very relevant to the quality of tandem mass spectra, and others may be not. In the next subsections, we introduce a sparse logistic regression model and a recursive feature elimination based on support vector machines (*SVM-RFE*) to select the most relevant features from those 69 introduced features.

### 3.2.5 Feature selection using sparse logistic regression

#### Logistic regression

Consider a training spectral dataset

$$\mathbf{X} = \{\mathbf{x}_i, y_i\}_{i=1}^N, \quad i = 1, \dots, N$$

$$\mathbf{x}_i \in R^D, y_i \in \{0, 1\}$$

where  $\mathbf{x}_i$  represents the  $i$ -th sample, a  $D$ -dimensional feature vector;  $y_i$  is the class label; and  $N$  is the number of training spectra. The logistic regression (LR) meth-

ods attempt to model the posterior probabilities of class memberships via logistic function of  $\mathbf{x}$ .

$$p(y = 1|\mathbf{x}, \mathbf{w}, w_0) = \sigma(\mathbf{w}^T \mathbf{x} + w_0) \quad (3.2)$$

where  $\sigma(\eta) = \frac{1}{1+e^{-\eta}}$  is the logistic function or sigmoid function,  $w_0$  is the intercept, and  $\mathbf{w} = (w_1, \dots, w_D)$  collects the coefficients.

More formally, the logistic regression model uses a Bernoulli model for the likelihood [Mur10, Alp04]. Therefore the likelihood is given by

$$p(y|\mathbf{x}, \mathbf{w}, w_0) = \sigma(\eta)^y (1 - \sigma(\eta))^{1-y} \quad (3.3)$$

where  $\eta = \mathbf{w}^T \mathbf{x} + w_0$ .

Assume that  $\mathbf{X}$  consists of  $N$  independent and identically distributed samples from a Bernoulli distribution, the negative log-likelihood function is given by

$$\begin{aligned} J(\mathbf{w}, w_0) &= - \sum_{i=1}^N \log p(y_i|\mathbf{x}_i, \mathbf{w}, w_0) \\ &= - \sum_{i=1}^N [y_i \log(\sigma(\eta_i)) + (1 - y_i) \log(1 - \sigma(\eta_i))] \end{aligned} \quad (3.4)$$

This negative log-likelihood function can be efficiently minimized by iterative gradient-based methods.

### Sparse logistic regression

The coefficients in Equation 3.4 corresponding to irrelevant features should be zeros and thus  $\mathbf{w}$  is a sparse vector. However, the resulting model obtained by minimizing the log-likelihood function Equation 3.4 may not be sparse. To get the sparse representation, an L1-regularization term is added to Equation 3.4 as a penalty. Thus we get the following L1-regularized objective function:

$$J(\mathbf{w}, w_0, \lambda) = - \sum_{i=1}^N \log p(y_i|\mathbf{x}_i, \mathbf{w}, w_0) + \lambda \|\mathbf{w}\|_1 \quad (3.5)$$

where  $\lambda$  is a positive scalar regularization parameter which controls the sparsity of the resulting model,  $\|\mathbf{w}\|_1 = \sum_i |w_i|$  is the 1-norm. The L1 regularization corresponds

to a Laplace prior, and this is a binary classification equivalence of Lasso [Tib96, Mur10]. The regularization parameter  $\lambda$  can be selected by cross validation or from a Bayesian approach [CT06]. Note that all components of  $\mathbf{w}$  are penalized equally by  $\lambda$ , so it is important that all components of  $\mathbf{w}$  are on the same scale. Therefore each feature is standardized with the mean of zero and the variance of one in this study.

To find  $\mathbf{w}$  and  $w_o$  which minimizes (3.5) is an active research area. There exist a large number of algorithms. Since the objective function (3.5) is convex, and the L1 norm is not differentiable, one can use generic methods for solving nondifferentiable convex problems. Recently, an efficient interior-point method was proposed [KKB07]. This algorithm takes truncated Newton steps and uses preconditioned conjugated gradient iterations. It can also produce high-precision solutions. Thus this algorithm is adopted as the sparse logistic regression solver.

### 3.2.6 Feature selection using SVM-RFE

#### Support vector machine

Support vector machines (*SVM*) were widely used years ago in statistical learning for solving classification and regression problems. Now it is becoming popular in a variety of biological applications [Nob06]. Here we briefly introduce *SVM* for the two-class classification problem which our problems belong to. A general discussion of *SVM* can be found in [Bis06, Vap98, Vap00, CST00, SS02].

For an *SVM* classifier, suppose that a training set composed of  $N$  spectral samples  $\mathbf{x}_i \in R^D$  with corresponding labels  $y_i \in \{-1, 1\}$  where  $i = 1, \dots, N$ . We assume that  $y_i \in \{-1, 1\}$  instead of  $\{0, 1\}$  as in logistic regression for the ease of discussion. In fact, we can convert  $\{-1, 1\}$  back to  $\{0, 1\}$  easily by a linear transformation.

If the original samples are not linear separable, the samples may become linear separable by introducing some nonlinear mapping to map a sample  $\mathbf{x}_i$  to  $\Phi(\mathbf{x}_i)$ , where  $\Phi(\mathbf{x})$  is a feature mapping [GS00], e.g.,

$$\Phi(\mathbf{x}) = (\mathbf{x}_1^2, \sqrt{2}\mathbf{x}_1\mathbf{x}_2, \mathbf{x}_2^2).$$

A unique optimal separating hyperplane (*OSH*) [HS01]

$$f(\mathbf{x}) = \mathbf{w}^T \Phi(\mathbf{x}) + b$$

can be constructed by maximizing the margin—the distance between the hyperplane and the nearest data points of each class. Maximizing the margin is equivalent to

$$\min \frac{1}{2} \|\mathbf{w}\|^2$$

subjecting to the constraint of

$$y_i(\mathbf{w}^T \Phi(\mathbf{x}) + b) \geq 1.$$

Note that we do not need to compute  $\Phi(\mathbf{x})$  for each training data point  $\mathbf{x}$  to find  $\mathbf{w}$  and  $b$  of the optimal hyperplane. Instead, for some nonlinear mappings, we can find a kernel which satisfies

$$k(\mathbf{x}_i, \mathbf{x}_j) = \Phi(\mathbf{x}_i)^T \Phi(\mathbf{x}_j)$$

and the problem of finding the optimal hyperplane can be done by only dot product computation in the feature space where the original samples are mapped to. Therefore, the dot product evaluation in feature space can be simplified to kernel function evaluation in the input space. This simplification is called the “kernel” technique [ABR64, SS02].

It is possible and desirable to find a hyperplane with large margin by allowing some samples been misclassified. This technique is called “soft margin” and is necessary in practice. For example, there may not exist a hyperplane which perfectly separates the data in feature space, or the margin may be too narrow. In these circumstances, the soft margin classifier is necessary to find a maximum margin classifier without causing overfitting.

To implement the soft margin classifier, a sample is penalized by

$$\zeta_i = |y_i - (\mathbf{w}^T \Phi(\mathbf{x}) + b)|$$

if the sample is misclassified or it is inside the margin boundary. The *OSH* [HS01] is then regarded as the solution of the optimization problem

$$\arg \min_{\mathbf{w}, b} C \sum_{i=1}^N \zeta_i + \frac{1}{2} \|\mathbf{w}\|^2$$

under constraints

$$y_i f(\mathbf{x}_i) \geq 1 - \zeta_i$$

where  $C > 0$  is a regularization parameter which controls the trade-off between the complexity of margin and misclassification error. The problem is a constrained optimization problem and can be solved by the use of Lagrange multipliers. The corresponding objective function is given in the next subsection. From the above discussion, we can see a support vector machine is essentially a kernelized maximum margin hyperplane classifier with soft margin.

### SVM-RFE algorithm

The recursive feature elimination based on support vector machine algorithm (*SVM-FRE*) is one of the backward elimination methods widely used for many problems [GWBV02, HS01, ZLS<sup>+</sup>06], but it has not been used for quality assessment of tandem mass spectra yet. This study will apply the *SVM-FRE* to select a set of the most relevant features for the purpose of quality assessment of spectra. Consider a set of  $N$  tandem mass spectra with their quality labels “-1” (for poor quality) or “1” (for high quality). Let  $D$  be the dimension of feature vectors. For spectrum  $i$  in the spectral dataset, let  $\mathbf{x}_i$  be a  $D$ -dimensional feature vector whose components are described in the previous subsection, and  $y_i$  be its quality label. The *SVM-RFE* recursively does the following steps.

Step 1. Train an *SVM* by solving the following quadratic optimization problem

$$\begin{aligned} \text{Minimize : } L(\mathbf{a}) &= - \sum_{i=1}^N a_i + \frac{1}{2} \sum_{i=1}^N \sum_{j=1}^N a_i a_j y_i y_j k(\mathbf{x}_i, \mathbf{x}_j) & (3.6) \\ \text{Subject to : } & \sum_{i=1}^N a_i y_i = 0, \text{ and } 0 \leq a_i \leq C, (i = 1, 2, \dots, N) \end{aligned}$$

where  $\mathbf{a} = \{a_1, a_2, \dots, a_N\}$  is a parameter vector to be found,  $C$  is a regularization parameter which controls the trade-off between misclassification errors and model complexity, and  $k(\mathbf{x}_i, \mathbf{x}_j)$  is a kernel function. The simplest kernel function is  $k(\mathbf{x}_i, \mathbf{x}_j) = \mathbf{x}_i^T \mathbf{x}_j$ , which is the linear kernel. Commonly used nonlinear kernel functions are radial basis functions, which are defined as  $k(\mathbf{x}_i, \mathbf{x}_j) = r(\|\mathbf{x}_i - \mathbf{x}_j\|^2)$

and  $r$  could be any nonnegative function. A typical radial basis kernel function is the Gaussian function  $k(\mathbf{x}_i, \mathbf{x}_j) = \exp(-\gamma\|\mathbf{x}_i - \mathbf{x}_j\|^2)$ , where  $\gamma$  is a nonnegative scalar.

Suppose  $\mathbf{a}^*$  solve the above quadratic optimization problem. Then the decision rule of *SVM*-based classification is given by  $\text{sign}(f(\mathbf{x}))$ , where

$$f(\mathbf{x}) = \sum_{i=1}^N a_i^* y_i k(\mathbf{x}, \mathbf{x}_i) + b^* \quad (3.7)$$

$$b^* = -\left(\max_{y_i=-1} \sum_{j=1}^N a_j y_j k(\mathbf{x}_i, \mathbf{x}_j) + \min_{y_i=1} \sum_{j=1}^N a_j y_j k(\mathbf{x}_i, \mathbf{x}_j)\right)/2$$

Step 2. For each feature  $k$  in a feature vector, calculate

$$d(k) = L(\mathbf{a}^*) - L_k(\mathbf{a}^*) \quad (3.8)$$

where  $L_k(\mathbf{a}^*)$  is computed by (3.6) using the  $(D - 1)$ -dimension feature vectors with the  $k$ -th feature removed from the  $D$ -dimension feature. To make computation trackable, the values of  $\mathbf{a}$  are assumed to be the same after the  $k$ -th feature is removed. Therefore there is no need to retrain a classifier after a feature is removed.

Step 3. Sort  $d(k)$ , and remove the feature whose corresponding value of  $d(k)$  is the smallest one. Because a feature is removed, the dimensionality of the remaining feature vector  $D = D - 1$ .

Step 4. Repeat doing Steps 1-3 above until a certain number of features have been selected, or the maximal value of  $d(k)$  calculated by (3.8) is significantly small.

The choice of kernel functions may affect the computational time and the performance of the *SVM* in the *SVM-RFE* method. For an *SVM* with the linear kernel function (called linear *SVM*), there is only one parameter  $C$ , and this parameter is relatively stable as the number of feature changes. While for an *SVM* with the nonlinear kernel function (called nonlinear *SVM*) such as Gaussian kernel, the parameter  $\gamma$  is sensitive to the number of feature used. However, a nonlinear *SVM* can perform better than a linear *SVM* in classifying spectra. Thus the features selected by using a nonlinear *SVM* may be more accurate if the parameters are the ‘‘optimal’’ ones for different features used.

To make a trade-off between accuracy and robustness, we adopt a two-stage *SVM-RFE* strategy for feature selection. First, a linear *SVM* is used to select



$D$  ( $D = 15$  in this study) most relevant features. Here the value of 15 for  $D$  is chosen according to the number of support vectors obtained after training an *SVM* classifier. Generally, when the number of support vectors becomes very large, this phenomena may indicate that overfitting is occurred or we have removed relevant features. Secondly, a nonlinear *SVM* with Gaussian kernel is used for ranking the  $D$  most relevant features.

Unlike the sparse logistic regression, the *SVM-RFE* algorithm may select redundant features. For the 69 constructed features, some of them are exactly the same. For this reason, we only retain one of the features which are exactly the same. After the process of removing the redundant features, only 61 features are left. We use the proposed two-stage *SVM-RFE* algorithm to select the most relevant features out of the 61 features.

The LIBSVM [CL01] is adopted as the *SVM* solver in this study. The hyper-parameters of *SVMs* are selected by a five-cross validation on the training data. For linear *SVM*, the parameter  $C$  is set to 0.08; for Gaussian kernel, the parameter  $C$  is set to 100, and  $\gamma$  is set to 0.08. For *SVM* classifiers, large  $C$  and  $\gamma$  may cause overfitting.

## 3.3 Results and discussion

### 3.3.1 Experimental datasets

This study employs two tandem mass spectral datasets: *ISB* dataset and *TOV* dataset to investigate the performance of the proposed method. The following is a brief description of these datasets.

(1) *ISB* dataset. This dataset consisting of 22 LC/MS/MS runs was produced by Institute of System Biology (*ISB*) from 18 control mixture proteins [KPN<sup>+</sup>02]. Tandem mass spectra in this dataset were searched using SEQUEST against a human protein database appended with sequences of the 18 control mixture proteins. This analysis produced 18,496 assignments to doubly charged spectra, 18,044 to triply

charged spectra, and 504 to singly charged spectra. After manual validation, 1656 peptide assignments to doubly charged spectra, 984 to triply charged spectra, and 132 to singly charged spectra were determined to be correct. These data were also analyzed by *InsPecT* which annotated another 820 possibly modified (mutated) peptides [TSF<sup>+</sup>05]. All these 3592 spectra are labeled as “high” quality, and all the other spectra in the dataset are labeled as “poor” quality in this study.

(2) *TOV* dataset. The data in *TOV* dataset consists of 22,576 ion trap spectra. These *MS/MS* spectra were searched against a subset of the Uniref100 database (release 1.2, <http://www.uniprot.org>) containing 44,278 human protein sequences using SEQUEST. This analysis produced 10,714 assignments to doubly charged spectra, 9732 to triply charged spectra, and 2430 to singly charged spectra. After validated by PeptideProphet [KNKA02], 1898 peptide assignments to doubly charged spectra, 261 to triply charged spectra, and 38 to singly charged spectra were determined to be correct (PeptideProphet scores equal or greater than 0.9). All these 2197 spectra are labeled as “high” quality in this study. All the other spectra in the dataset are labeled as “poor” quality.

### 3.3.2 Training and performance evaluation

The effectiveness of the proposed feature selection method is evaluated by comparing the performance of the classifiers trained with different set of features. We first divide the *ISB* dataset into two equal size subsets: one for feature selection and classifier training, the other for classifier testing. Each subset has the same number of high quality spectra and poor quality spectra. It is expected that the most relevant features selected based on the *ISB* dataset can be applicable to other datasets to train superior classifiers. To do this we also divide the *TOV* dataset into two equal size subsets as for the *ISB* dataset. One subset is used to train classifiers with the features selected based on the *ISB* dataset, while the other subset is used to evaluate the performance of the classifiers.

For the evaluation of the performance of the trained classifiers, we reported true positive rates (*TPR*, the fraction of positives correctly classified as positives) and

false positive rates ( $FPR$ , the fraction of negatives misclassified as positives). We also reported receiver operating characteristic ( $ROC$ ) curves [Faw04], which are a plot of  $TPR$  as a function of  $FPR$ . The  $ROC$  curve is very useful to view a classifier’s performance and tune a classifier to have a fixed  $TPR$  or true negative rate ( $TNR$ , the fraction of negatives correctly classified as negatives and  $TNR = 1 - FPR$ ). For the unbalanced data which have different number of positives and negatives, to tune a classifier is very important. The area under the curve ( $AUC$ ) was used for comparing classification results. The  $AUC$  is 1 for perfect classification and 0.5 just the same as random guess.

### 3.3.3 Feature selected by SLR and the classification results

To select the truly highly relevant features and remove the false positives, we construct several subsets of the training data, and run L1-regularized logistic regression on the subsets. The final selected features are the intersect of the multiple runs. To do this, a number of training subsets are constructed from the training data for feature selection. These training subsets can be constructed by bootstrap resampling [Efr79, HMM<sup>+</sup>05]. However, for tandem mass spectrum data, the numbers of high quality and poor quality spectra are highly biased. For this reason, we first extract the high quality spectra from the training subset, then we randomly draw the same number of poor quality spectra from the training subset. This processing is repeated 25 times, and we get 25 subsets for feature selection.

Figure 3.2 shows the selection frequency (top panel) and the absolute values of the mean weights of the 69 features (bottom panel). The more frequently the features are selected, the more likely the features are highly relevant because these features are not likely selected by chance. In addition, the features with large weights are more likely to be relevant features than those with small weights because the features with large weights will contribute significantly to compute the posterior probability in logistic models. From Figure 3.2, we can see that the more frequently selected features also have larger weights than the less selected features in general. Therefore, in this study the features occur 80% of times (i.e., 20 times) are selected. By using

this threshold, 10 features are selected out of the 69 features. These 10 features and their meanings are listed in Table 3.2. The results agree with our prior knowledge. For example, the features which represent the existence of pairs of ions whose mass differences equal to the masses of the 20 amino acids are selected. As we know, these features are relevant features and are used by *de-novo* peptide identification algorithms.

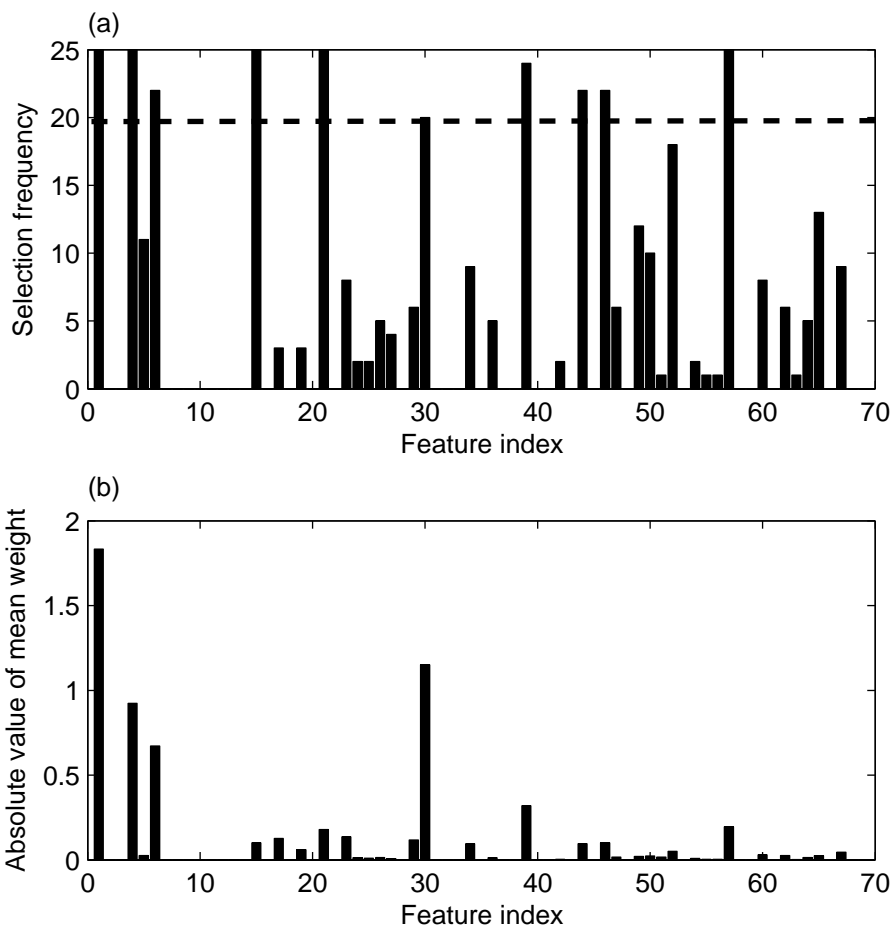


**Figure 3.2:** (a) The feature selection frequency and (b) the absolute values of mean weights in the twenty-five runs.

To test the effectiveness of the selected features, a logistic regression classifier is trained using only the 10 selected features. Table 3.3 shows the performance of the classifier in terms of the *AUC* and *TNR*. In [WSCC07], logistic regression was also used for quality assessment of tandem mass spectra, and the results were very good.

**Table 3.2:** The selected features by the *SLR* model and the meanings of the selected features.

Index	Feature meanings
$W_1$	Amino acid distance (singly charged)
$W_4$	Complementary ions (singly charged)
$W_6$	Complementary ions (multiply charged)
$B_3$	Good-Diff Fraction
$N_1$	$x_{rea}$
$S_9$	Total intensity of $b_{n-1}$ ion
$\hat{W}_8$	Water loss
$F_4$	Average delta mass in spectra
$F_6$	Charge of precursor ions
$F_{17}$	Total intensity of complementary pairs

In their study, logistic regression classifier was used to classify tandem mass spectra based on nine features. In this study, we also construct their nine features, and construct a logistic regression model for quality assessment of tandem mass spectra. The results are also shown in Table 3.3.

**Table 3.3:** Compare the overall classification results using different features selected by the *SLR* model in terms of *AUC* and *TNR* at a fixed true positive rate of 90%.

Features	<i>ISB</i>		<i>TOV</i>	
	<i>AUC</i>	<i>TNR</i>	<i>AUC</i>	<i>TNR</i>
Wong's	0.88	73.79%	0.90	76.45%
Selected	<b>0.93</b>	<b>80.48%</b>	<b>0.95</b>	<b>85.06%</b>

From the classification results shown in Table 3.3, the performance of classifiers based on the selected ten features is better than that based on the nine features constructed in [WSCC07]. The results indicate the proposed sparse logistic regression method can successfully select the highly relevant features.

Because some features are highly redundant, and some features are exactly the same, ordinary logistic regression may be numerically unstable. For this reason, we do not report the classification results based on the whole 69 features.

The L1 regularized logistic regression method also has some shortcomings. Firstly, for the colinear features, the sparse logistic regression methods may randomly select one of them. Secondly, since logistic regression is a generalized linear classifier, further improvement may be achieved by using nonlinear methods for feature selection, such as nonlinear support vector machines which is the topic of the next subsection.

### 3.3.4 Features selected by SVM-RFE and the classification results

For the *ISB* dataset, Table 3.4 lists the top 15 most relevant features selected by the proposed two-stage *SVM-RFE* algorithm. From the definition of the features in Section 3.2.4, we can see that the features are not independent. For example,  $B_5, F_7, W_4$  are correlated because they all reflect some aspects of the presence of pairs of complementary fragment ions whose masses sum up to the mass of the precursor ion. However, they are not redundant because they combined have more discriminative power than a feature alone. The selected features also show that the presence of complementary fragment ions combined with the mass of the precursor ion ( $B_5, F_7, W_4$ ) is very important to predict the quality of spectra. In fact, for peptide identification algorithms such as Mascot, the mass tolerances of the precursor ion and the fragment ion significantly influence the number of identified peptides. The presence of fragment ions differing by the mass of one of the 20 amino acids ( $W_1, B_3$ ) is also an important feature to predict the quality of spectra. The peaks with mass difference equal to the mass of an amino acid are the basis of *de-novo* peptide identification algorithms. The presence of water or ammonia loss peaks, the presence of *CO* group losing peaks, and  $y_{n-2}$  peaks are also relevant features. These peaks are also taken into consideration to design peptide identification algorithms. Some global features ( $F_4, F_5, \hat{W}_4$ ) which reflect the overall attribute of a spectrum

are also relevant to predict the quality of spectra, such as the mean and standard deviation of mass difference. Most of these features have not directly been used for designing peptide identification algorithms such as Mascot and SEQUEST. However, some researchers have used these features to identify false positives and false negatives after a database search [FMV<sup>+</sup>06, WSCC07].

**Table 3.4:** The relative importance of the 15 most relevant features ranked using a nonlinear *SVM-RFE*

Index	Feature meanings
$B_5$	The total intensity of complimentary pairs
$F_7$	The mass of uncharged precursor
$W_1$	Amino acid distance (singly charged)
$F_4$	The average delta mass in a spectrum
$B_3$	The Good-Diff Fraction
$W_4$	Complementary ions (singly charged)
$W_7$	The presence of water or ammonia losing peaks (single charged)
$\hat{W}_4$	The ratio of significant peaks
$F_5$	The standard deviation of delta mass values
$W_{10}$	The presence of <i>CO</i> or <i>NH3</i> losing peaks (singly charged)
$S_7$	The total intensity of $y_{n-2}$ ion
$W_{11}$	The presence of <i>CO</i> or <i>NH3</i> losing peaks (doubly charged)
$\hat{N}_4$	The number of sequence tag of length one (wighted)
$\hat{N}_3$	The number of sequence tag of length one
$F_9$	The relative intensity of the precursor

For different number of features used, the classification results for the *ISB* dataset are shown in Table 3.5. We can see that a small number of features can improve the classification accuracy. Thus the selected features are effective because these features are highly relevant features with which we can better predict the quality of spectra.

To test whether the features selected based on one dataset are also good to predict the quality of spectra in another dataset, the features selected from the *ISB* dataset

are directly applied to train a classifier for the *TOV* training data. Then the trained classifier is used to predict spectral quality of the *TOV* testing data. The results are also given in Table 3.5. From Table 3.5, it is clear that the classification results are similar, which means the features selected are stable and can be used to predict the quality of spectra obtained from ion trap spectrometers.

**Table 3.5:** Compare the overall classification results using different number of features selected by the *SVM-RFE* algorithm for both *ISB* and *TOV* datasets. When we report true negative rate (*TNR*) ( $TNR = 1 - FPR$ ), the *TPR* is fixed at 90%, so  $TNR = 91.50\%$  means that we can filter out 91.50% of poor quality spectra and only lose 10% of high quality spectra.

#	<i>ISB</i>		<i>TOV</i>	
	<i>AUC</i>	<i>TNR</i>	<i>AUC</i>	<i>TNR</i>
61	0.9411	87.62%	0.9490	87.53%
15	0.9632	91.50%	0.9624	91.65%
13	<b>0.9656</b>	92.09%	0.9645	92.60%
11	0.9640	<b>92.62%</b>	0.9652	<b>92.89%</b>
9	0.9635	92.19%	0.9657	92.59%
7	0.9608	91.79%	<b>0.9673</b>	<b>92.89%</b>
5	0.9478	86.73%	0.9527	89.12%

The two-stage *SVM-RFE* method can select the highly relevant features to describe the quality of spectra. The results of experiments with the *ISB* dataset have illustrated that the presented method can effectively select the most relevant features in terms of performance of the *SVMs* trained with the selected features and the all available features. Furthermore, the *SVMs* are trained for the *TOV* dataset with the selected features based on *ISB* dataset and the all available features. The comparison of performances of *SVMs* has shown that the *SVM* with the selected features is better than the *SVM* with the all available features. It is also observed that the *SVMs* with the selected features only based on *ISB* dataset perform equally well for both *ISB* and *TOV* datasets. This may indicate that the selected features



reflect the intrinsic property of tandem mass spectra.

### 3.4 The most relevant feature set

So far, we have presented an *SLR* model and a two-stage *SVM-RFE* method to select the most relevant features to describe the quality of spectra. Clearly, the features selected by using the two methods are different. For example, among the ten most relevant features, only four features are the same. They are  $W_1, W_3, B_3$  and  $F_4$ . Therefore we should find out which feature set is more relevant to the quality of tandem mass spectra. To do this, *SVM* classifiers are trained on the 10 most relevant features selected by the *SLR* model and *SVM-RFE*, respectively. *LR* models are also trained on the 10 most relevant features selected based on the two feature selection methods. The results are given in Table 3.6. From the classification results shown in Table 3.6, the features selected via the two-stage *SVM-RFE* algorithm seems better than the features selected via the *SLR* model.

**Table 3.6:** Compare the relevance of the two feature sets selected by the *SLR* model and the *SVM-RFE* algorithm.

Classifier	Feature selection	<i>ISB</i>		<i>TOV</i>	
		<i>AUC</i>	<i>TNR</i>	<i>AUC</i>	<i>TNR</i>
<i>LR</i>	<i>SLR</i>	0.9311	80.48%	0.9505	85.06%
<i>LR</i>	<i>SVM-RFE</i>	0.9374	81.82%	0.9563	90.12%
<i>SVM</i>	<i>SVM-RFE</i>	<b>0.9635</b>	<b>91.31%</b>	<b>0.9673</b>	<b>92.57%</b>
<i>SVM</i>	<i>SLR</i>	0.9469	87.48%	0.9587	91.03%

# CHAPTER 4

## CLUSTERING ANALYSIS FOR MASS SPECTRUM QUALITY ASSESSMENT

### 4.1 Introduction

In the past, several supervised machine learning algorithms have been proposed to assess the quality of tandem mass spectra. For supervised machine learning, a labeled training dataset is needed to train a classifier, and the trained classifier is used to classify spectra as high quality or poor quality. Ideally, the spectra of the training set should be identified by several peptide identification algorithms and manually validated, i.e., the set should be correctly labeled without or with very few falsely labeled spectra. However, such spectral data sets are hard to obtain in most cases. Worse still, tandem mass spectrometers may produce different spectra even for the same peptide under different experimental conditions. Therefore, the training and testing spectra may not come from the same probability distribution and the trained classifier may fail to discriminate poor quality spectra from high quality ones. The performance of classifiers can be improved by training a specific classifier for each experiment. On the other hand, clustering algorithms, which do not need a training set, may be alternative choices for the quality assessment of tandem mass spectra.

In this chapter, we use clustering algorithms to cluster the experimental spectra without using any prior information about the spectral dataset from search engines. The remainder of this chapter is organized as follows. Section 4.2 introduces the model based clustering algorithm. In Section 4.3, the *ISB* and the *TOV* datasets are used to investigate the performance of the algorithm. The experimental results

show the model based clustering algorithm can remove about 57.64% and 66.36% of poor quality spectra while losing only 10% of high quality spectra for the two tandem mass spectral datasets: *ISB* and *TOV* dataset, respectively.

## 4.2 Clustering analysis

### 4.2.1 Background

Contrast to supervised learning methods, the unsupervised learning methods do not need a labeled training set. Several types of unsupervised learning methods are widely used. The first type of methods is density estimation which estimates the underlying probability density function  $P(X)$  of a given dataset  $X$ . The second type of methods is dimension reduction methods such as principle component analysis, independent component analysis, and multidimensional scaling. The third type of methods is clustering [Fuk90, HTF01, Mur10].

Clustering is the assignment of data to different groups so that data in the same group are more similar than those in different groups [HTF01, JMF99]. Clustering is a difficult problem since no prior information about the data is given. Therefore we need to make some assumptions to solve the clustering problems. For example, the  $k$ -means algorithm assumes data can be grouped into spherical and nearly the same size clusters [Mac67]. The model based clustering methods assume that data are generated from a predefined statistical model. Since different definitions of the clustering can result in different clusters, there is no single best clustering algorithm. Accordingly, the definition of clustering is at the heart of clustering algorithm design [Web02, Fuk90].

According to the different definitions of clustering, the existing clustering methods can be classified as combinatorial, model based and mode seeking algorithms [HTF01, JMF99]. Combinatorial algorithms do not assume a probability distribution on the data, and samples are assigned to clusters by optimizing an objective function [Mac67, SM00, FD07]. Contrary to combinatorial methods, the statistical

model based methods assume samples are independent and identically distributed from a predefined probability density function such as mixture of Gaussian distributions. After inferring the unknown parameters, clustering is achieved by assigning samples to different Gaussian components [Bil98, DLR77]. When the assumed probabilistic distribution is correct, the model based algorithm may achieve good clustering results. The mode seeking methods take a nonparametric approach to find the modes of the probability density function of data, and a sample is assigned to its nearest mode [HTF01, CM02]. The mode seeking methods may be good choices if the structure of data is very complex and can't be modeled by a simple parametric probability distribution.

The existing clustering methods can also be classified as hierarchical and partitional clustering. For hierarchical clustering, a hierarchical tree can be constructed in two ways: bottom-up and top-down. At the beginning, the bottom-up hierarchical clustering method views a single point as a group. The two most similar groups are merged successively until all the data are merged into a single cluster [Web02]. Alternatively, the top-down hierarchical clustering method successively splits groups until each group has only one single point. Hierarchical clustering is pretty useful when the data can be described by a tree. However, the hierarchical tree is not stable, a small change in data may change the tree completely. Partitional clustering, on the other hand, divides the data into disjoint clusters. Thus the final clusters are flat. In the following, we will use a partitional clustering algorithm – a model based clustering algorithm for the quality assessment of tandem mass spectra. This algorithm is a parametrical method since it assumes a predefined probability distribution of spectral feature data.

### 4.2.2 Model based clustering for quality assessment

After exploratory data analysis and from previous research [BGM04, WGD08], the distribution of high quality spectra and poor quality spectra can be modeled by

a mixture of Gaussian distributions:

$$p(\mathbf{x}) = \sum_{k=1}^K \pi_k \mathcal{N}(\mathbf{x}|\mu_k, \Sigma_k) \quad (4.1)$$

where  $K$  is the number of mixture components and here  $K = 2$ ; one component corresponds to high quality spectra while the other component corresponds to poor quality spectra.  $\pi_k$  is the mixture coefficient.  $\mathcal{N}(\mathbf{x}|\mu_k, \Sigma_k)$  is a Gaussian density function with its mean of  $\mu_k$  and covariance matrix of  $\Sigma_k$ , and  $\mathbf{x}$  is a feature vector. For this study, we use the *EM* (expectation maximization) algorithm (see below) to estimate the parameters of the Gaussian mixture model [Bil98].

To use the *EM* algorithm for parameter estimation, we need to provide the initial guess of the parameters. Here the  $k$ -means algorithm is used to initialize the *EM* algorithm [Mac67, AV07].

### ***K*-means**

*K*-means (also known as C-means) is a kind of combinational algorithm. For given unlabeled feature vectors  $\mathbf{x}_n \in R^D$  ( $n = 1, \dots, N$ ), we want to partition the  $N$  data points into  $K$  clusters. The exhaustive search is not practical because there are approximately  $\frac{N^K}{K!}$  possible partitions. Alternatively, an objective function can be defined to measure the quality of a partition so the partition problem can be formulated as minimizing the objective function. To define the objective function, we first introduce a set of  $D$ -dimensional vectors  $\mu_k$  which is a prototype associated with the  $k^{th}$  cluster, where  $k = 1, \dots, K$  [Bis06]. For each data point  $\mathbf{x}_n$ , we introduce a set of indicator variables  $r_{nk} \in \{0, 1\}$ . If  $\mathbf{x}_n$  is assigned to cluster  $k$  then  $r_{nk} = 1$ , and  $r_{ni} = 0$  for  $i \neq k$ . Now we can define the objective function as follows:

$$J = \sum_{n=1}^N \sum_{k=1}^K r_{nk} \|\mathbf{x}_n - \mu_k\|^2. \quad (4.2)$$

Our goal is to find the  $r_{nk}$  and  $\mu_k$  to minimize the objective function. Directly optimizing the function is *NP*-hard while the *K*-means provides a smart way to optimize it.

The  $K$ -means is an alternative optimization algorithm. Given initial prototype  $\mu_k$ , we first minimize  $J$  with respect to  $r_{nk}$ , keeping  $\mu_k$  fixed. Because  $J$  is a linear function with respect to  $r_{nk}$ , we only need to assign each data point to the closest prototype. In the second step, we optimize  $J$  with respect to  $\mu_k$ , keeping  $r_{nk}$  fixed. Setting the partial derivative of  $J$  with respect to  $\mu_k$  to zero gives  $2 \sum_{n=1}^N r_{nk}(\mathbf{x}_n - \mu_k) = 0$ . Now we can get  $\mu_k = \frac{\sum_n r_{nk} \mathbf{x}_n}{\sum_n r_{nk}}$ . So the second step assigns sample mean to each prototype.  $K$ -means repeats the above two steps until the prototypes do not change.

The  $K$ -means is a competitive learning algorithm. The  $K$  clusters compete with each other for the right to own the data points [Mac03]. It is very efficient and can be used to initialize other algorithms. It always converges in a finite number of steps, yet may find a local minimum of the objective function (4.2).  $K$ -means does not provide posterior probabilities for the assignment of spectra to clusters because it simply assigns points to the nearest cluster. On the contrary, the  $EM$  algorithm provides posterior probabilities.

## EM algorithm

For Gaussian mixture models, it is difficult to use the maximum likelihood estimation of the parameters because there exists a summation over  $k$  that occurs inside a logarithm for the log-likelihood function. However, we can introduce a latent variable  $\mathbf{z}$  which is the label of  $\mathbf{x}$ . Here  $\mathbf{z}$  is a  $K$ -dimensional latent variable. The value of the  $k$ -th component of  $\mathbf{z}$  satisfy  $z_k \in \{0, 1\}$  and  $\sum_{k=1}^K z_k = 1$ . The distribution of  $\mathbf{z}$  is specified by the mixture coefficients

$$p(z_k = 1) = \pi_k \quad (4.3)$$

The joint distribution of  $\mathbf{x}$  and  $\mathbf{z}$  is

$$p(\mathbf{x}, \mathbf{z}) = p(\mathbf{x}|\mathbf{z})p(\mathbf{z}) = \prod_{k=1}^K \mathcal{N}(\mathbf{x}|\mu_k, \Sigma_k)^{z_k} \pi_k^{z_k} \quad (4.4)$$

The posterior probability of  $\mathbf{z}$  given  $\mathbf{x}$  is

$$p(\mathbf{z}|\mathbf{x}) = \frac{\prod_{k=1}^K \mathcal{N}(\mathbf{x}|\mu_k, \Sigma_k)^{z_k} \pi_k^{z_k}}{\sum_{\mathbf{z}_k} \prod_{k=1}^K \mathcal{N}(\mathbf{x}|\mu_k, \Sigma_k)^{z_k} \pi_k^{z_k}} \quad (4.5)$$

Note that only one  $k$  makes  $z_k = 1$ . Thus

$$p(z_k = 1|\mathbf{x}) = \frac{\mathcal{N}(\mathbf{x}|\mu_k, \Sigma_k)\pi_k}{\sum_{k=1}^K \mathcal{N}(\mathbf{x}|\mu_k, \Sigma_k)\pi_k} \quad (4.6)$$

Suppose that we are given data  $\mathbf{X}$  which is an  $N \times D$  matrix. The  $n$ -th row  $\mathbf{x}_n^T$  is a feature vector which represents the quality of the  $n$ -th spectrum. The corresponding latent variable matrix is  $\mathbf{Z}$ , which is an  $N \times K$  indicator matrix and the value of  $z_{nk}$  satisfies  $z_{nk} \in \{0, 1\}$  and  $\sum_{k=1}^K z_{nk} = 1$ .

Given  $\mathbf{X}$  and  $\mathbf{Z}$ , the likelihood function of  $\mu, \Sigma, \pi$  becomes

$$p(\mathbf{X}, \mathbf{Z}|\mu, \Sigma, \pi) = \prod_{n=1}^N \prod_{k=1}^K \mathcal{N}(\mathbf{x}_n|\mu_k, \Sigma_k)^{z_{nk}} \pi_k^{z_{nk}} \quad (4.7)$$

The log-likelihood function becomes

$$\ln p(\mathbf{X}, \mathbf{Z}|\mu, \Sigma, \pi) = \sum_{n=1}^N \sum_{k=1}^K z_{nk} (\ln \mathcal{N}(\mathbf{x}_n|\mu_k, \Sigma_k) + \ln \pi_k) \quad (4.8)$$

Now suppose that we already know  $\mu_k^i, \Sigma_k^i, \pi_k^i$ , then the posterior distribution for  $z_{nk}$  is ( $E$ -step)

$$p(z_{nk} = 1|\mathbf{x}_n, \mu_k^i, \Sigma_k^i, \pi_k^i) = \frac{\pi_k^i \mathcal{N}(\mathbf{x}_n|\mu_k^i, \Sigma_k^i)}{\sum_{k=1}^K \pi_k^i \mathcal{N}(\mathbf{x}_n|\mu_k^i, \Sigma_k^i)} \quad (4.9)$$

Now compute the score function

$$\begin{aligned} Q &= \sum_{z_{nk}} \ln p(\mathbf{X}, \mathbf{Z}|\mu, \Sigma, \pi) p(z_{nk} = 1|\mathbf{x}_n, \mu_k^i, \Sigma_k^i, \pi_k^i) \\ &= \sum_{n=1}^N \sum_{k=1}^K p(z_{nk} = 1|\mathbf{x}_n, \mu_k^i, \Sigma_k^i, \pi_k^i) (\ln \mathcal{N}(\mathbf{x}_n|\mu_k, \Sigma_k) + \ln \pi_k) \end{aligned} \quad (4.10)$$

Maximizing  $Q$  under the constraint of  $\sum_{k=1}^K \pi_k = 1$  by the use of Lagrange multiplier, we get ( $M$ -step)

$$\begin{aligned} N_k &= \sum_{n=1}^N p(z_{nk} = 1|\mathbf{x}_n, \mu_k^i, \Sigma_k^i, \pi_k^i) \\ \pi_k^{i+1} &= \frac{N_k}{N} \end{aligned} \quad (4.11)$$

$$\mu_k^{i+1} = \frac{1}{N_k} \sum_{n=1}^N p(z_{nk} = 1|\mathbf{x}_n, \mu_k^i, \Sigma_k^i, \pi_k^i) \mathbf{x}_n \quad (4.12)$$

$$\Sigma_k^{i+1} = \frac{1}{N_k} \sum_{n=1}^N p(z_{nk} = 1|\mathbf{x}_n, \mu_k^i, \Sigma_k^i, \pi_k^i) (\mathbf{x}_n - \mu_k^{i+1})(\mathbf{x}_n - \mu_k^{i+1})^T \quad (4.13)$$

Given initial values for  $\pi$ ,  $\mu$  and  $\Sigma$ , the *EM* algorithm alternates between the *E*-step and the *M*-step, and finally find a local maximum of the incomplete likelihood function (integrate out  $\mathbf{Z}$  in Equation (4.8) ).

## 4.3 Results and discussion

### 4.3.1 The clustering results of the EM algorithm

The *EM* algorithm has been run 10 times on *ISB* and *TOV* datasets described in previous chapters. The clustering results are shown in Table 4.1. The *TNRs* are calculated as *TPRs* are fixed at 90% in Table 4.1. In the experiments, we use the top 10 features selected by the *SVM-RFE* algorithm described in Chapter 3. The proposed clustering algorithm can remove about 66.36% of poor quality spectra while losing about 10% of interpretable spectra for the spectra of the *TOV* dataset. While for the spectra of the *ISB* dataset, about 57.64% of poor quality spectra can be safely removed without losing more than 10% of high quality spectra.

Table 4.2 shows the clustering results for the threshold of zero, i.e., a spectrum is assigned to the cluster with the larger posterior probability. Even using this simple threshold, about 53.47% ( $= 17853/(17853 + 15599)$ ) of poor quality spectra can be removed while losing only 6.26% of high quality spectra for the spectra of *ISB* dataset. For the spectra of *TOV* dataset, about 53.73% ( $= 10949/(9430 + 10949)$ ) of poor quality spectra can be removed while losing only 3.41% ( $= 75/(2122 + 75)$ ) of high quality spectra. In other words, more than 53% of poor quality spectra can be removed by using the zero threshold while very minority of high quality spectra are lost.

### 4.3.2 The salient features for EM algorithm

The relevant features for classification may have little power for clustering methods to discriminate poor quality spectra from high quality ones. For this reason, we want to find the discriminative features for the *EM* clustering algorithm. We call



**Table 4.1:** The clustering results of the *EM* algorithm. The *EM* algorithm has been run 10 times, and the *AUC* and *TNR* are nearly the same for *ISB* dataset. For *TOV* dataset, the results show the *EM* algorithm converged to three local maxima.

Experiments	<i>ISB</i>		<i>TOV</i>	
	<i>AUC</i>	<i>TNR</i>	<i>AUC</i>	<i>TNR</i>
1	0.7647	57.64%	0.8214	66.33%
2	0.7647	57.64%	0.8214	66.33%
3	0.7647	57.64%	0.8214	66.33%
4	0.7647	57.64%	0.8214	66.36%
5	0.7647	57.64%	0.8214	66.33%
6	0.7647	57.64%	0.8214	66.36%
7	0.7647	57.64%	0.8214	66.36%
8	0.7647	57.64%	<b>0.8592</b>	<b>58.32%</b>
9	0.7647	57.64%	0.8214	66.33%
10	0.7647	57.64%	0.8214	66.36%

**Table 4.2:** The distribution of spectra in different clusters with the threshold of zero. For *ISB* dataset, the numbers are the average of the 10 runs. For *TOV* dataset, the numbers are the average of 9 runs (excluding the 8-*th* run)

Dataset	Predicted High Quality	Predicted Poor Quality
<i>ISB</i>		
High Quality	3367	225
Poor Quality	15599	17853
<i>TOV</i>		
High Quality	2122	75
Poor Quality	9430	10949

these salient features, which may be found from the cluster centers of the *EM* algorithm. Since each feature is normalized to have mean of zero and variance of one, the features with large absolute values between centers may be salient features for cluster analysis.

Table 4.3 lists the cluster centers from the 10 runs of the *EM* algorithm. For *ISB* dataset, the numbers are the average of the 10 runs. For *TOV* dataset, the numbers are the average of 9 runs (excluding the 8-*th* run). From the clustering centers of each dataset, some features have nearly the same values in both clusters while other potential salient features’s values are quite different. These potential salient features are highlighted in Table 4.3.

**Table 4.3:** The clustering centers of the *EM* algorithm. The potential salient features are highlighted. The majority of spectra in cluster one are high quality spectra while those in cluster two are poor quality spectra.

Feature	<i>ISB</i>		<i>TOV</i>	
	Clustering one	Clustering two	Clustering one	Clustering two
<b>B<sub>5</sub></b>	<b>0.51</b>	<b>-0.54</b>	<b>0.60</b>	<b>-0.63</b>
<i>F<sub>7</sub></i>	-0.20	0.21	0.07	-0.07
<b>W<sub>1</sub></b>	<b>0.54</b>	<b>-0.57</b>	<b>0.65</b>	<b>-0.69</b>
<i>F<sub>4</sub></i>	0.00	0.00	0.46	-0.48
<i>B<sub>3</sub></i>	0.04	-0.04	-0.31	0.33
<b>W<sub>4</sub></b>	<b>0.49</b>	<b>-0.51</b>	<b>0.54</b>	<b>-0.57</b>
<b>W<sub>7</sub></b>	<b>0.56</b>	<b>-0.59</b>	<b>0.67</b>	<b>-0.70</b>
<b><math>\hat{W}_4</math></b>	<b>-0.84</b>	<b>0.89</b>	<b>-0.77</b>	<b>0.81</b>
<i>F<sub>5</sub></i>	-0.11	0.12	0.37	-0.39
<b>W<sub>10</sub></b>	<b>0.53</b>	<b>-0.55</b>	<b>0.63</b>	<b>-0.66</b>

Figure 4.1 plots the absolute values of feature differences between two cluster centers in descending order. For *ISB* dataset, from Figure 4.1 (a), the four features with small absolute values of feature difference may be discarded because their values

are far smaller compared to other six features. For *TOV* dataset, the cluster center differences do not show a distinct partition line compared to those of *ISB* dataset but they show a similar trend of decrease. The *EM* algorithm has been applied to the dimension reduced feature sets in which only the six features with large absolute values of cluster center difference are retained. The clustering results are given in Table 4.4, and the results are better than those using the whole 10 features.

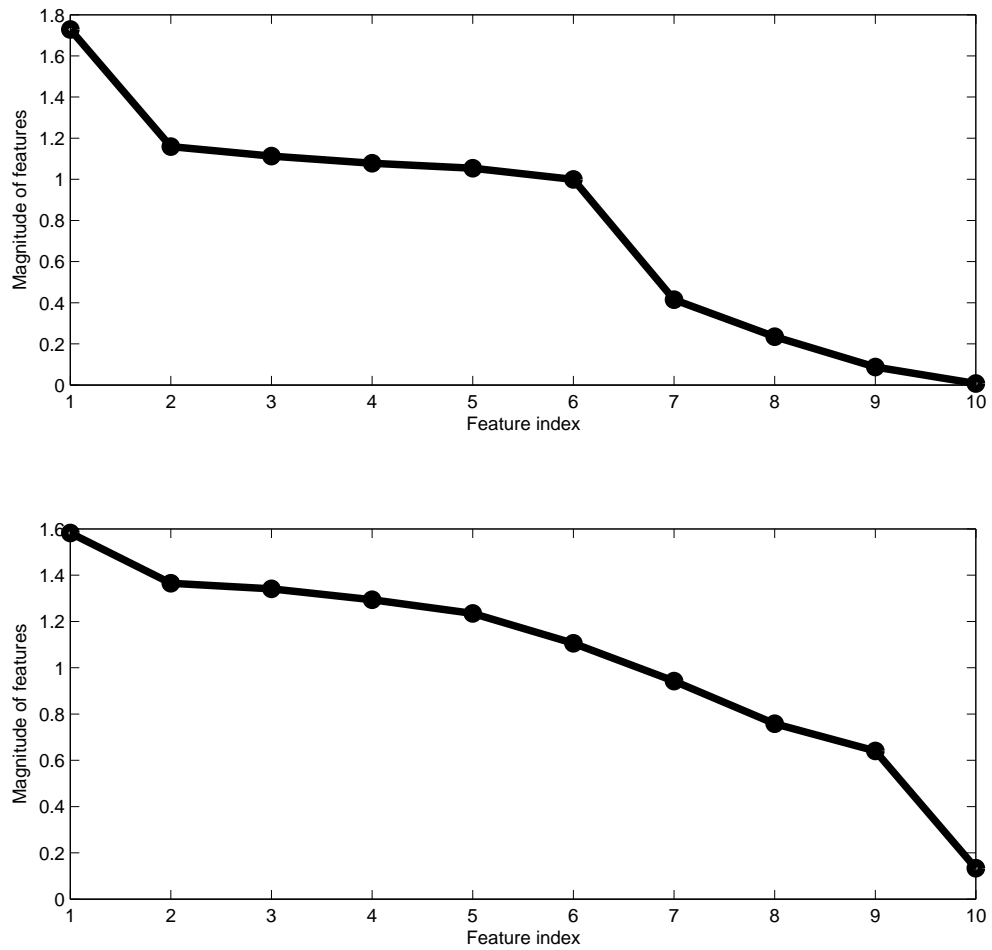


**Figure 4.1:** Plot of the absolute values of clustering center difference in descending order for *ISB* dataset (a) and *TOV* dataset (b).

**Table 4.4:** The clustering results of the *EM* algorithm using the six salient features.

Experiments	<i>ISB</i>		<i>TOV</i>	
	<i>AUC</i>	<i>TNR</i>	<i>AUC</i>	<i>TNR</i>
1	0.7674	58.16%	0.8290	66.99%
2	0.7675	58.16%	0.8290	66.99%
3	0.7674	58.16%	0.8289	66.87%
4	0.7674	58.16%	0.8214	66.36%
5	0.7674	58.16%	0.8290	66.99%
6	0.7674	58.16%	0.8290	66.99%
7	0.7674	58.16%	0.8290	66.99%
8	0.7674	58.16%	0.8290	66.99%
9	0.7674	58.16%	0.8290	66.99%
10	0.7674	58.16%	0.8290	66.99%

### 4.3.3 Determine the quality of spectra in each cluster

From the cluster centers, we can easily determine the spectra in which cluster are high quality or poor quality. From the definition of  $B_5$ ,  $W_1$ ,  $W_4$ ,  $W_7$  and  $W_{10}$ , the high quality spectra should have larger value for these features than for poor quality spectra. In cluster one, the values of these features are larger than those in cluster two.  $\hat{W}_4$  is the ratio of the number of peaks which have a relative intensity greater than 1% of the total intensity to the total number of peaks in a spectrum. For this feature, it is a bit difficult to image whether the high quality spectra should have larger values or not. For this reason, we compute the mean for both the high quality and poor quality spectra of this feature in *ISB* dataset, and the values are  $-0.77$  and  $0.08$ , respectively. Clearly, the high quality spectra have smaller values for this feature. For both *ISB* and *TOV* datasets, the value of  $\hat{W}_4$  in cluster one is smaller than that in clustering two. The above experimental results may show the mixture of Gaussian distribution is a reasonable model of the spectral feature data.

# CHAPTER 5

## CONCLUSIONS AND FUTURE WORK

### 5.1 Conclusions

In this thesis, we have applied several methods for the pre-processing of tandem mass spectra. Firstly, since about 80% of peaks in a spectrum are noisy peaks, a novel denoising algorithm is used to filter most noisy peaks. After denoised by the proposed algorithm, about 69% of peaks in a spectrum can be removed. At the same time, the number of spectra that can be identified by Mascot search engine increases by 31.23% and 14.12% for the spectra from two datasets *ISB* and *TOV*, respectively.

Secondly, in addition to the noise in spectra, most spectra produced by tandem mass spectrometers are poor quality spectra and they can't be identified by peptide identification algorithms. Removing these poor quality spectra before peptide identification can save the time for identifying these uninterpretable spectra, and decrease false positive rates in peptide identifications. We use machine learning algorithms for the quality assessment of tandem mass spectra. To enable learning, each spectrum is represented by a fixed length feature vector. The challenging task for machine learning is to find the discriminative features which can best differentiate the high quality spectra from the poor quality ones. Therefore, we have designed several feature selection algorithms to select these discriminative relevant features. These algorithms include a two-stage recursive feature elimination based on support vector machine and a sparse logistic regression model. Experimental results show that supervised machine learning algorithms such as support vector machine can be trained to remove more than 90% of poor quality spectra without losing more than

10% of high quality spectra.

Thirdly, a labeled training set is needed for supervised machine learning algorithms. However, the spectra produced from the same peptide under different experimental conditions may be quite different, so the supervised machine learning algorithms' performance may be degenerated if the training and testing spectra are from different experiments or different tandem mass spectrometers. We use model-based clustering algorithms for quality assessment of tandem mass spectra without the need of a training dataset. Experiments have shown that more than 53% of poor quality spectra can be safely removed at the expense of removing very minority of high quality spectra (about 6.26% and 3.41% of high quality spectra of two datasets *ISB* and *TOV*, respectively).

These pre-processing methods improve the reliability of peptide identification from tandem mass spectra, thus more information can be extracted from tandem mass spectra. At the same time, as most noisy peaks of spectra and poor quality spectra are removed, the resources for storing the spectra and the time for identifying the processed spectra are also decreased, even dramatically, e.g., about 70% of storage space can be saved after the spectra are denoised by the proposed method in Chapter 2 of this thesis.

## 5.2 Future work

Based on the workflow proposed in Chapter 1, we have designed several algorithms to pre-process tandem mass spectra. By the implementation of the algorithms in the proposed workflow, for an input experimental spectrum, we can output the quality label of the spectrum as well as the denoised version of this spectrum. However, in the present workflow, we have not explored the relationship between some modules. For example, we have not shown the influence of denoising to feature extraction, then to feature selection and finally to quality assessment. There is a great need to do so since the denoised spectra have far less peaks than the original undenoised spectra, and thus denoising spectra can speed up or even help constructing discriminate

features.

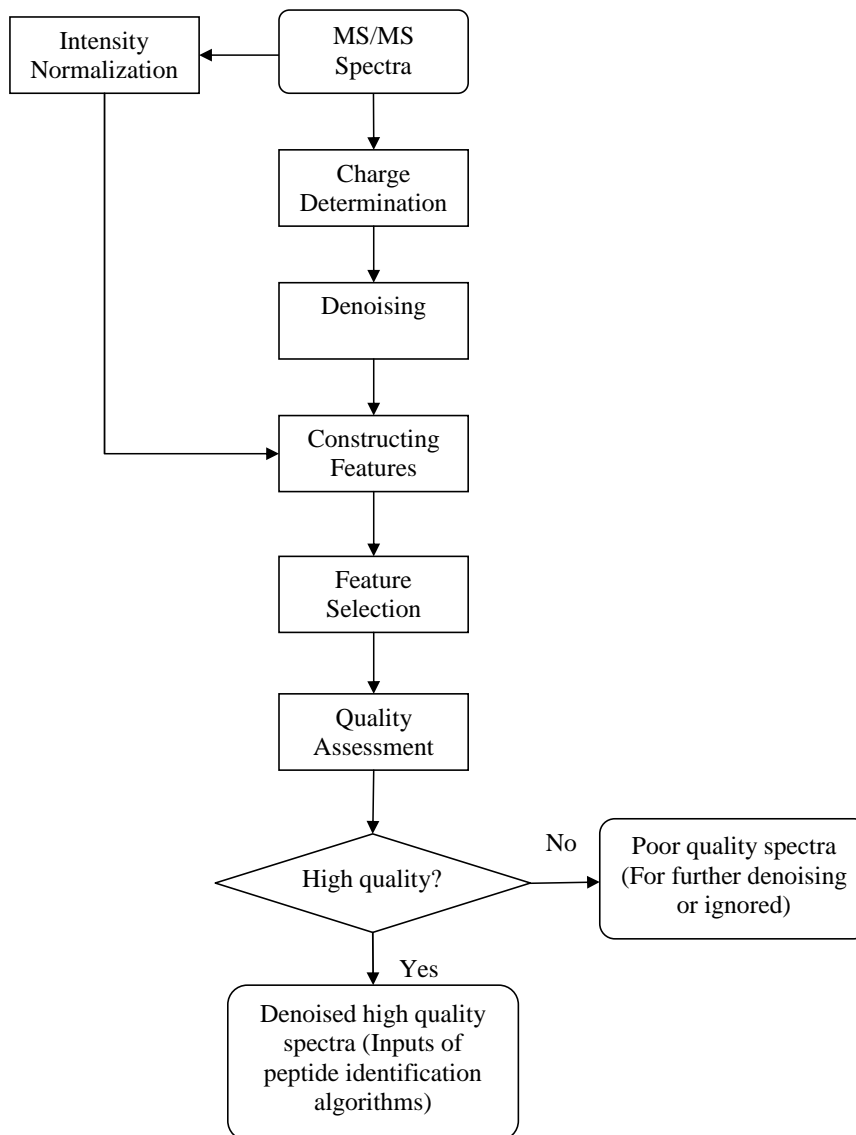


**Figure 5.1:** The new workflow for pre-processing tandem mass spectra

As we have stated in Chapter 1, common pre-processing methods include spectrum clustering, precursor charge state determination, spectral intensity normalization, denosing and quality assessment of tandem mass spectra. We have conducted some research on precursor charge state determination [ZDSW08]. Because of the limitation of time, I can't conduct enough experiments and thus do not add charge state determination to our workflow. However, charge state determination is very important because it can influence both denosing and quality assessment. For spec-

trum clustering, it is difficult to be implemented online. Consequently, it is also not integrated into our workflow.

To improve our present workflow, we proposed the new workflow shown in Figure 5.1. In this workflow, the charge state determination and the filtering model is critical since the subsequent modules are based on the outputs of these modules.

Note that some modules in the workflow can also be used as post-processing methods for peptide identifications. For example, the uninterpretable spectra from peptide identification algorithms can be denoised and then be used for further identification. For quality assessment algorithms, they can be used to find false negatives, false positives or post-translational peptides.



## REFERENCES

- [ABR64] M.A. Aizerman, E.M. Braverman, and L.I. Rozonoer. Theoretical foundations of the potential function method in pattern recognition learning. *Automation and remote control*, 25:821–837, 1964.
- [Alp04] E. Alpaydin. *Introduction to machine learning*. MIT press, 2004.
- [AM02] C. Ambroise and G.J. McLachlan. Selection bias in gene extraction on the basis of microarray gene-expression data. *Proceedings of the National Academy of Sciences*, 99(10):6562, 2002.
- [AM03] R. Aebersold and M. Mann. Mass spectrometry-based proteomics. *Nature*, 422:198–207, 2003.
- [AV07] D. Arthur and S. Vassilvitskii. K-means++: The advantages of careful seeding. In *Proceedings of the eighteenth annual ACM-SIAM symposium on Discrete algorithms*, pages 1027–1035. Society for Industrial and Applied Mathematics Philadelphia, PA, USA, 2007.
- [BCG<sup>+</sup>02] S. Baginsky, M. Cieliebak, W. Gruissem, T. Kleffmann, Z. Liptak, M. Muller, and P. Penna. AuDeNS: a tool for automatic de novo peptide sequencing. *Technical Report no 383, ETH Zurich, Dept of Computer Science*, 2002.
- [BCG07] M. Bern, Y. Cai, and D. Goldberg. Lookup peaks: a hybrid of de novo sequencing and database search for protein identification by tandem mass spectrometry. *Anal. Chem.*, 79(4):1393–1400, 2007.
- [BE01] V. Bafna and N. Edwards. SCOPE: a probabilistic model for scoring tandem mass spectra against a peptide database. *Bioinformatics*, 17(suppl 1):S13–S21, 2001.
- [BGM<sup>+</sup>04] M. Bern, D. Goldberg, W.H. McDonald, and J.R. Yates. Automatic quality assessment of peptide tandem mass spectra. *Bioinformatics*, 20(s1):i49–i54, 2004.
- [Bil98] J.A. Bilmes. A gentle tutorial of the EM algorithm and its application to parameter estimation for Gaussian mixture and hidden Markov models. Technical Report ICSI-TR-97-02, University of Berkeley, 1998.
- [Bis06] C.M. Bishop. *Pattern recognition and machine learning*. Springer, 2006.

- [BLY<sup>+</sup>07] B.M. Balgley, T. Laudeman, L. Yang, T. Song, and C.S. Lee. Comparative Evaluation of Tandem MS Search Algorithms Using a Target-Decoy Search Strategy. *Molecular & Cellular Proteomics*, 6(9):1599–1608, 2007.
- [Bre98] L. Breiman. *Classification and regression trees*. Chapman & Hall/CRC, 1998.
- [BTBP04] N. Bandeira, H. Tang, V. Bafna, and P. Pevzner. Shotgun protein sequencing by tandem mass spectra assembly. *Anal. Chem.*, 76(24):7221–7233, 2004.
- [CB04] R. Craig and R.C. Beavis. TANDEM: matching proteins with tandem mass spectra. *Bioinformatics*, 20(9):921–922, 2004.
- [Cha] D.H. Chace. A layperson’s guide to tandem mass spectrometry and newborn screening. <http://www.savebabies.org/NBS/msms-chace.php>.
- [CL01] C.C. Chang and C.J. Lin. *LIBSVM: a library for support vector machines*, 2001. Software available at <http://www.csie.ntu.edu.tw/~cjlin/libsvm>.
- [CM02] D. Comaniciu and P. Meer. Mean shift: a robust approach toward feature space analysis. *IEEE Transactions on Pattern Analysis and Machine Intelligence*, 24(5):603–619, 2002.
- [CMD<sup>+</sup>03] J. Colinge, J. Magnin, T. Dessingy, M. Giron, and A. Masselot. Improved peptide charge state assignment. *Proteomics*, 3(8):1434–1440, 2003.
- [CMG<sup>+</sup>03] J. Colinge, A. Masselot, M. Giron, T. Dessingy, and J. Magnin. OLAV: Towards high-throughput tandem mass spectrometry data identification. *Proteomics*, 3(8):1454–1463, 2003.
- [CST00] N. Cristianini and J. Shawe-Taylor. *An introduction to support Vector Machines: and other kernel-based learning methods*. Cambridge Univ. Pr., 2000.
- [CT06] G.C. Cawley and N.L.C. Talbot. Gene selection in cancer classification using sparse logistic regression with Bayesian regularization. *Bioinformatics*, 22(19):2348–2355, 2006.
- [CT07] K.W. Choo and W.M. Tham. Tandem mass spectrometry data quality assessment by self-convolution. *BMC bioinformatics*, 8(1):352, 2007.
- [DAC<sup>+</sup>99] V. Dancik, T.A. Addona, K.R. Clauser, J.E. Vath, and P.A. Pevzner. De novo peptide sequencing via tandem mass spectrometry. *Journal of Computational Biology*, 6(3-4):327–342, 1999.

- [DB04] J.G. Dy and C.E. Brodley. Feature selection for unsupervised learning. *The Journal of Machine Learning Research*, 5:845–889, 2004.
- [DCSL02] M. Dash, K. Choi, P. Scheuermann, and H. Liu. Feature selection for clustering—a filter solution. In *Proceedings of the 2002 IEEE International Conference on Data Mining (ICDM'02)*, pages 115–122. IEEE Computer Society Washington, DC, USA, 2002.
- [DHS00] R.O. Duda, P.E. Hart, and D.G. Stork. *Pattern classification*. Wiley-Interscience, 2000.
- [DLR77] A.P. Dempster, N.M. Laird, and D.B. Rubin. Maximum likelihood from incomplete data via the EM algorithm. *Journal of the Royal Statistical Society. Series B (Methodological)*, 39(1):1–38, 1977.
- [DR05] K. Duan and J.C. Rajapakse. SVM-RFE peak selection for cancer classification with mass spectrometry data. *Proc. 3rd Asia-Pacific Bioinf. Conf.*, 1:191–200, 2005.
- [DSPW09] J. Ding, J. Shi, G.G. Poirier, and F.X. Wu. A novel approach to denoising tandem mass spectra. *Proteome Science*, 7(9), 2009.
- [DSW09] J. Ding, J. Shi, and F.X. Wu. Quality assessment of tandem mass spectra by using a weighted k-means. *Clinical Proteomics*, 2009. Accepted.
- [DSZW08] J. Ding, J. Shi, A.M. Zou, and F.X. Wu. Feature selection for tandem mass spectrum quality assessment. In *IEEE International Conference on Bioinformatics and Biomedicine (IEEE BIBM 2008)*, pages 310–313, 2008.
- [DW09a] J. Ding and F.X. Wu. Feature selection for tandem mass spectrum quality assessment via sparse logistic regression. In *The 3rd International Conference on Bioinformatics and Biomedical Engineering (iCBBE 2009)*, 2009. Accepted.
- [DW09b] J. Ding and F.X. Wu. Model based clustering for quality assessment of tandem mass spectra. 2009. In preparation.
- [Efr79] B. Efron. Bootstrap methods: another look at the jackknife. *The Annals of Statistics*, 7(1):1–26, 1979.
- [EHFG05] J.E. Elias, W. Haas, B.K. Faherty, and S.P. Gygi. Comparative evaluation of mass spectrometry platforms used in large-scale proteomics investigations. *Nat. Methods*, 2(9):667–675, 2005.
- [EMY94] J.K. Eng, A.L. McCormack, and J.R. Yates. An approach to correlate tandem mass spectral data of peptides with amino acid sequences in a protein database. *J. Am. Soc. Mass Spectrom.*, 5(11):976–989, 1994.

- [FA05] J. Falkner and P. Andrews. Fast tandem mass spectra-based protein identification regardless of the number of spectra or potential modifications examined. *Bioinformatics*, 21(10):2177–2184, 2005.
- [Faw04] T. Fawcett. ROC graphs: notes and practical considerations for researchers. *Machine Learning*, 31, 2004.
- [FBS<sup>+</sup>08] A.M. Frank, N. Bandeira, Z. Shen, S. Tanner, S.P. Briggs, R.D. Smith, and P.A. Pevzner. Clustering millions of tandem mass spectra. *J. Proteome Res.*, 7(1):113–122, 2008.
- [FD07] B.J. Frey and D. Dueck. Clustering by passing messages between data points. *Science*, 315(5814):972–976, 2007.
- [FMH<sup>+</sup>07] K. Flikka, J. Meukens, K. Helsens, J. Vandekerckhove, I. Eidhammer, K. Gevaert, and L. Martens. Implementation and application of a versatile clustering tool for tandem mass spectrometry data. *Proteomics*, 7(18):3245–3258, 2007.
- [FMV<sup>+</sup>06] K. Flikka, L. Martens, J. Vandekerckhove, K. Gevaert, and I. Eidhammer. Improving the reliability and throughput of mass spectrometry-based proteomics by spectrum quality filtering. *Proteomics*, 6(7):2086–2094, 2006.
- [FNC07] J. Feng, D.Q. Naiman, and B. Cooper. Probability model for assessing proteins assembled from peptide sequences inferred from tandem mass spectrometry data. *Anal. Chem*, 79(10):3901–3911, 2007.
- [FP05] A. Frank and P. Pevzner. PepNovo: de novo peptide sequencing via probabilistic network modeling. *Anal. Chem.*, 77(4):964–973, 2005.
- [FRR<sup>+</sup>05] B. Fischer, V. Roth, F. Roos, J. Grossmann, S. Baginsky, P. Widmayer, W. Gruissem, and J.M. Buhmann. NovoHMM: a hidden Markov model for de novo peptide sequencing. *Anal. Chem.*, 77(22):7265–7273, 2005.
- [Fuk90] K. Fukunaga. *Introduction to Statistical Pattern Recognition*. Academic Press, 1990.
- [GGNZ06] I. Guyon, S. Gunn, M. Nikravesh, and L.A. Zadeh. *Feature extraction: foundations and applications (studies in fuzziness and soft computing)*. Springer, 2006.
- [GKPW03] M. Gentzel, T. Kocher, S. Ponnusamy, and M. Wilm. Preprocessing of tandem mass spectrometric data to support automatic protein identification. *Proteomics*, 3(8):1597–1610, 2003.
- [GMK<sup>+</sup>04] L.Y. Geer, S.P. Markey, J.A. Kowalak, L. Wagner, M. Xu, D.M. Maynard, X. Yang, W. Shi, and S.H. Bryant. Open mass spectrometry search algorithm. *Journal of Proteome Research*, 3(5):958–964, 2004.

- [GRC<sup>+</sup>05] J. Grossmann, F.F. Roos, M. Cieliebak, Z. Liptak, L.K. Mathis, M. Muller, W. Gruissem, and S. Baginsky. AUDENS: a tool for automated peptide de novo sequencing. *J. Proteome Res.*, 4(1):768–771, 2005.
- [GS00] I. Guyon and D.G. Stork. *Advances in large margin classifiers*, chapter Linear discriminant and support vector classifiers, pages 147–169. MIT Press, 2000.
- [GSM03] B. Georgescu, I. Shimshoni, and P. Meer. Mean shift based clustering in high dimensions: a texture classification example. *Proceedings of the Ninth IEEE International Conference on Computer Vision (ICCV’03)*, pages 456–463, 2003.
- [Gue08] S. Guerif. Unsupervised Variable Selection: when random rankings sound as irrelevancy. *JMLR: Workshop and Conference Proceedings*, 4:163–177, 2008.
- [GW07] R.C. Gonzalez and R.E. Woods. *Digital image processing*. Prentice Hall, 2007.
- [GWBV02] I. Guyon, J. Weston, S. Barnhill, and V. Vapnik. Gene selection for cancer classification using support vector machines. *Machine Learning*, 46(1):389–422, 2002.
- [HCM<sup>+</sup>08] T. Hesterberg, N. Choi, L. Meier, ETH Zuerich, C. Fraley, et al. Least angle and L 1 penalized regression: A review. volume 2, pages 61–93. American Statistical Association, 2008.
- [HCN05] X. He, D. Cai, and P. Niyogi. Laplacian score for feature selection. *Advances in Neural Information Processing Systems*, 18, 2005.
- [HK08] M. Hilario and A. Kalousis. Approaches to dimensionality reduction in proteomic biomarker studies. *Briefings in Bioinformatics*, 9(2):108–118, 2008.
- [HKPM06] M. Hilario, A. Kalousis, C. Pellegrini, and M. Muller. Processing and classification of protein mass spectra. *Mass Spectrometry Reviews*, 25(3), 2006.
- [HMA06] P. Hernandez, M. Muller, and R.D. Appel. Automated protein identification by tandem mass spectrometry: Issues and strategies. *Mass Spectrometry Reviews*, 25(2):235–254, 2006.
- [HMM<sup>+</sup>05] T. Hesterberg, S. Monaghan, D.S. Moore, A. Clipson, and R. Epstein. *The practice of business statistics, (fifth edition)*, chapter Bootstrap methods and permutation tests. 2005.

- [HS01] S. Hua and Z. Sun. Support vector machine approach for protein sub-cellular localization prediction. *Bioinformatics*, 17(8):721–728, 2001.
- [HTF01] T. Hastie, R. Tibshirani, and J. Friedman. *The elements of statistical learning: data mining, inference, and prediction*. Springer, 2001.
- [Hun93] L. Hunter. *Artificial Intelligence and Molecular Biology*, chapter Molecular biology for computer scientists, pages 1–46. MIT Press, 1993.
- [HZM00] D.M. Horn, R.A. Zubarev, and F.W. McLafferty. Automated de novo sequencing of proteins by tandem high-resolution mass spectrometry, 2000.
- [JMF99] AK Jain, MN Murty, and PJ Flynn. Data clustering: a review. *ACM computing surveys*, 31(3):264–323, 1999.
- [JP04] N.C. Jones and P. Pevzner. *An introduction to bioinformatics algorithms*. MIT Press Cambridge, Mass, 2004.
- [KHG08] J. Khatun, E. Hamlett, and M.C. Giddings. Incorporating sequence information into the scoring function: a hidden Markov model for improved peptide identification. *Bioinformatics*, 24(5):674–681, 2008.
- [KKB07] K. Koh, S.J. Kim, and S. Boyd. An interior-point method for large-scale L1-regularized logistic regression. *Journal of Machine Learning Research*, 8:1519–1555, 2007.
- [KL07] N. Kang and H.W. Leong. Algorithm for peptide sequencing by tandem mass spectrometry based on better preprocess and anti-symmetric computational model. *Proceedings of the 2007 IEEE Computational Systems Bioinformatics Conference (CSB'07)*, 2007.
- [KNKA02] A. Keller, A.I. Nesvizhskii, E. Kolker, and R. Aebersold. Empirical statistical model to estimate the accuracy of peptide identifications made by MS/MS and database search. *Anal. Chem.*, 74(20):5383–5392, 2002.
- [KPN+02] A. Keller, S. Purvine, AI Nesvizhskii, S. Stolyar, DR Goodlett, and E. Kolker. Experimental protein mixture for validating tandem mass spectral analysis. *OMICS*, 6(2):207–212, 2002.
- [KS00] M. Kinter and N.E. Sherman. *Protein sequencing and identification using tandem mass spectrometry*. Wiley, 2000.
- [KSC+05] E.A. Kapp, F. Schutz, L.M. Connolly, J.A. Chakel, J.E. Meza, C.A. Miller, D. Fenyo, J.K. Eng, J.N. Adkins, G.S. Omenn, et al. An evaluation, comparison, and accurate benchmarking of several publicly available MS/MS search algorithms: sensitivity and specificity analysis. *Proteomics*, 5(13):3475–3490, 2005.

- [KWMN05] AA Klammer, CC Wu, MJ MacCoss, and WS Noble. Peptide charge state determination for low-resolution tandem mass spectra. In *Proceedings of the IEEE Computational Systems Bioinformatics Conference (CSB 2005)*, pages 175–185, 2005.
- [LBB<sup>+</sup>07] J. Liu, A.W. Bell, J.J.M. Bergeron, C.M. Yanofsky, B. Carrillo, C.E.H. Beaudrie, and R.E. Kearney. Methods for peptide identification by spectral comparison. *Proteome Science*, 5(3), 2007.
- [LFJ04] MHC Law, MAT Figueiredo, and AK Jain. Simultaneous feature selection and clustering using mixture models. *IEEE Transactions on Pattern Analysis and Machine Intelligence*, 26(9):1154–1166, 2004.
- [LM98] H. Liu and H. Motoda. *Feature selection for knowledge discovery and data mining*. Springer, 1998.
- [LM07] H. Liu and H. Motoda. *Computational methods of feature selection*. Chapman & Hall/CRC, 2007.
- [LTK<sup>+</sup>04] R.D. LeDuc, G.K. Taylor, Y.B. Kim, T.E. Januszyk, L.H. Bynum, J.V. Sola, J.S. Garavelli, and N.L. Kelleher. ProSight PTM: an integrated environment for protein identification and characterization by top-down mass spectrometry. *Nucleic Acids Research*, 32(suppl 2):W340–W345, 2004.
- [LZN08] L. Li, J. Zhang, and R.M. Neal. A method for avoiding bias from feature selection with application to Naive Bayes classification models. *Bayesian Analysis*, 3(1):171–196, 2008.
- [Mac67] J.B. MacQueen. Some methods for classification and analysis of multivariate observations. In *Proceedings of the fifth Berkeley symposium on mathematical statistics and probability*, pages 281–297. University of California Press, 1967.
- [Mac03] D.J.C. MacKay. *Information theory, inference, and learning algorithms*. Cambridge University Press New York, 2003.
- [Mal99] S. Mallat. *A wavelet tour of signal processing*. Academic press, 1999.
- [MH08] S. Ma and J. Huang. Penalized feature selection and classification in bioinformatics. *Briefings in Bioinformatics*, 9(5):392–403, 2008.
- [MMP02] P. Mitra, CA Murthy, and SK Pal. Unsupervised feature selection using feature similarity. *IEEE Transactions on Pattern Analysis and Machine Intelligence*, 24(3):301–312, 2002.
- [MRH<sup>+</sup>06] N. Mujezinovic, G. Raidl, JR Hutchins, J.M. Peters, K. Mechtler, and F. Eisenhaber. Cleaning of raw peptide MS/MS spectra: improved protein identification following deconvolution of multiply charged peaks,

- isotope clusters, and removal of background noise. *Proteomics*, 6(19):5117–5131, 2006.
- [MS90] P. Maragos and RW Schafer. Morphological systems for multidimensional signal processing. *Proceedings of the IEEE*, 78(4):690–710, 1990.
- [Mur10] K. Murphy. *Machine learning: a probabilistic approach*. MIT Press, 2010. In preparation.
- [MZH<sup>+</sup>03] B. Ma, K. Zhang, C. Hendrie, C. Liang, M. Li, A. Doherty-Kirby, and G. Lajoie. PEAKS: powerful software for peptide de novo sequencing by tandem mass spectrometry. *Rapid communications in mass spectrometry*, 17(20):2337–2342, 2003.
- [MZL05] B. Ma, K. Zhang, and C. Liang. An effective algorithm for peptide de novo sequencing from MS/MS spectra. *Journal of Computer and System Sciences*, 70(3):418–430, 2005.
- [Nob06] W.S. Noble. What is a support vector machine? *Nature Biotechnology*, 24(12):1565–1567, 2006.
- [NP06] S. Na and E. Paek. Quality assessment of tandem mass spectra based on cumulative intensity normalization. *J. Proteome Res.*, 5(12):3241–3248, 2006.
- [NPL08] S. Na, E. Paek, and C. Lee. CIFTER: automated charge-state determination for peptide tandem mass spectra. *Anal. Chem.*, 80(5):1520–1528, 2008.
- [NRG<sup>+</sup>06] A.I. Nesvizhskii, F.F. Roos, J. Grossmann, M. Vogelzang, J.S. Eddes, W. Gruissem, S. Baginsky, and R. Aebersold. Dynamic spectrum quality assessment and iterative computational analysis of shotgun proteomic data toward more efficient identification of post-translational modifications, sequence polymorphisms, and novel peptides. *Molecular & Cellular Proteomics*, 5(4):652–670, 2006.
- [NTV<sup>+</sup>05] C. Narasimhan, D.L. Tabb, N.C. VerBerkmoes, M.R. Thompson, R.L. Hettich, and E.C. Uberbacher. MASPIC: intensity-based tandem mass spectrometry scoring scheme that improves peptide identification at high confidence. *Anal. Chem.*, 77(23):7581–7593, 2005.
- [NVA07] A.I. Nesvizhskii, O. Vitek, and R. Aebersold. Analysis and validation of proteomic data generated by tandem mass spectrometry. *Nature methods*, 4(10):787–797, 2007.
- [PKK04] S. Purvine, N. Kolker, and E. Kolker. Spectral quality assessment for high-throughput tandem mass spectrometry proteomics. *Omics A Journal of Integrative Biology*, 8(3):255–265, 2004.



- [PPDC99] D.N. Perkins, D.J.C Pappin, Creasy D.M., and J.S. Cottrell. Probability-based protein identification by searching sequence databases using mass spectrometry data. *Electrophoresis*, 20(18):3551–3567, 1999.
- [RCA<sup>+</sup>04] T. Rejtar, H.S. Chen, V. Andreev, E. Moskovets, and B.L. Karger. Increased identification of peptides by enhanced data processing of high-resolution MALDI TOF/TOF mass spectra prior to database searching. *Anal. Chem.*, 76(20):6017–6028, 2004.
- [RD06] A.E. Raftery and N. Dean. Variable selection for model-based clustering. *Journal of the American Statistical Association*, 101(473):168–178, 2006.
- [RGE03] A. Rakotomamonjy, I. Guyon, and A. Elisseeff. Variable selection using SVM-based criteria. *Journal of Machine Learning Research*, 3:1357–1370, 2003.
- [SAdP08] Y. Saeys, T. Abeel, and YV de Peer. Towards robust feature selection techniques. In *Proceedings of Benelearn*, pages 45–46, 2008.
- [SED<sup>+</sup>02] R.G. Sadygov, J. Eng, E. Durr, A. Saraf, H. McDonald, M.J. MacCoss, and J.R. Yates III. Code developments to improve the efficiency of automated MS/MS spectra interpretation. *Journal of Proteome Research*, 1(3):211–215, 2002.
- [SHH08] R.G. Sadygov, Z. Hao, and A.F.R. Huhmer. Charger: combination of signal processing and statistical learning algorithms for precursor charge-state determination from electron-transfer dissociation spectra. *Anal. Chem*, 80(2):376–386, 2008.
- [SIL07] Y. Saeys, I. Inza, and P. Larranaga. A review of feature selection techniques in bioinformatics. *Bioinformatics*, 23(19):2507–2517, 2007.
- [SM00] J. Shi and J. Malik. Normalized cuts and image segmentation. *IEEE Transactions on Pattern Analysis and Machine Intelligence*, 22(8):888–905, 2000.
- [SMF<sup>+</sup>06] J. Salmi, R. Moulder, J.J. Filen, O.S. Nevalainen, T.A. Nyman, R. Laheesmaa, and T. Aittokallio. Quality classification of tandem mass spectrometry data. *Bioinformatics*, 22(4):400–406, 2006.
- [SS02] B. Scholkopf and A.J. Smola. *Learning with kernels*. MIT press Cambridge, Mass, 2002.
- [SYI03] R.G. Sadygov and J.R. Yates III. A hypergeometric probability model for protein identification and validation using tandem mass spectral data and protein sequence databases. *Anal. Chem*, 75(15):3792–3798, 2003.

- [TEYI01] D.L. Tabb, J.K. Eng, and J.R. Yates III. Protein Identification by SEQUEST. *Proteome Research: Mass Spectrometry (James, P. ed.)*, pages 125–142, 2001.
- [Tib96] R. Tibshirani. Regression shrinkage and selection via the lasso. *Journal of the Royal Statistical Society*, 58(issue 1):267–288, 1996.
- [TMW<sup>+</sup>03] D.L. Tabb, M.J. MacCoss, C.C. Wu, S.D. Anderson, and J.R. Yates. Similarity among tandem mass spectra from proteomic experiments: detection, significance, and utility. *Anal. Chem.*, 75(10):2470–2477, 2003.
- [TSF<sup>+</sup>05] S. Tanner, H. Shu, A. Frank, L. Wang, E. Zandi, M. Mumby, P.A. Pevzner, and V. Bafna. Inspect: fast and accurate identification of post-translationally modified peptides from tandem mass spectra. *Anal. Chem.*, 77(14):4626–4639, 2005.
- [TSS<sup>+</sup>06] D.L. Tabb, M.B. Shah, M.B. Strader, H.M. Connelly, R.L. Hettich, and G.B. Hurst. Determination of peptide and protein ion charge states by Fourier transformation of isotope-resolved mass spectra. *Journal of the American Society for Mass Spectrometry*, 17(7):903–915, 2006.
- [TZH07] Y. Tang, Y.Q. Zhang, and Z. Huang. Development of two-stage SVM-RFE gene selection strategy for microarray expression data analysis. *IEEE/ACM Transactions on Computational Biology and Bioinformatics*, 4(3):365–381, 2007.
- [Vap98] V.N. Vapnik. *Statistical learning theory*. Wiley New York, 1998.
- [Vap00] V.N. Vapnik. *The nature of statistical learning theory*. Springer, 2000.
- [VGLH06] R. Varshavsky, A. Gottlieb, M. Linial, and D. Horn. Novel unsupervised feature filtering of biological data. *Bioinformatics*, 22(14), 2006.
- [Vin93] L. Vincent. Morphological grayscale reconstruction in image analysis: applications and efficient algorithms. *IEEE Transactions on Image Processing*, 2(2):176–201, 1993.
- [WDP08] F.X. Wu, J. Ding, and G.G. Poirier. An approach to assess peptide mass spectral quality without prior information. *International Journal of Functional Informatics and Personalised Medicine*, 5(2):140–155, 2008.
- [Web02] A. Webb. *Statistical pattern recognition*. Wiley-Interscience, 2002.
- [WGDP06] F-X. Wu, P. Gagne, A. Droit, and G-G. Poirier. RT-PSM, a real-time program for peptide-spectrum matching with statistical significance. *Rapid communications in mass spectrometry*, 20(8):1199–1208, 2006.
- [WGDP08] F.X. Wu, P. Gagne, A. Droit, and G.G. Poirier. Quality assessment of peptide tandem mass spectra. *BMC Bioinformatics*, 9(suppl:6):S13, 2008.

- [WSCC07] J.W.H. Wong, M.J. Sullivan, H.M. Cartwright, and G. Cagney. msm-sEval: tandem mass spectral quality assignment for high-throughput proteomics. *BMC Bioinformatics*, 8(1), 2007.
- [WTE07] X Wu, C.W. Tsebg, and N. Edwards. HMMatch: peptide identification by spectral matching of tandem mass spectra using hidden Markov models. *Journal of Computational biology*, 14(8), 2007.
- [WYC06] Y. Wan, A. Yang, and T. Chen. PepHMM: a hidden Markov model based scoring function for mass spectrometry database search. *Anal. Chem.*, 78(2):432–437, 2006.
- [XGB<sup>+</sup>05] M. Xu, L.Y. Geer, S.H. Bryant, J.S. Roth, J.A. Kowalak, D.M. Maynard, and S.P. Markey. Assessing data quality of peptide mass spectra obtained by quadrupole ion trap mass spectrometry. *J. Proteome Res.*, 4(2):300–305, 2005.
- [ZAS02] N. Zhang, R. Aebersold, and B. Schwikowski. ProbID: a probabilistic algorithm to identify peptides through sequence database searching using tandem mass spectral data. *Proteomics*, 2(10):1406–1412, 2002.
- [ZDSW08] A.M. Zou, J. Ding, J Shi, and F.X. Wu. Charge state determination of peptide tandem mass spectra using support vector machine (SVM). In *Proceedings of the 8th IEEE International Conference on Bioinformatics and Bioengineering (BIBE 2008)*, 2008.
- [ZHL<sup>+</sup>08] J. Zhang, S. He, CX Ling, X. Cao, R. Zeng, and W. Gao. PeakSelect: preprocessing tandem mass spectra for better peptide identification. *Rapid communications in mass spectrometry*, 22(8):1203–1212, 2008.
- [ZL07] Z. Zhao and H. Liu. Semi-supervised feature selection via spectral analysis. In *Proceedings of the 2007 SIAM International Conference on Data Mining*, pages 641–646, 2007.
- [ZLS<sup>+</sup>06] X. Zhang, X. Lu, Q. Shi, XQ Xu, HC Leung, L.N. Harris, J.D. Iglehart, A. Miron, J.S. Liu, and W.H. Wong. Recursive SVM feature selection and sample classification for mass-spectrometry and microarray data. *BMC Bioinformatics*, 7(1):S13, 2006.
- [ZSZ<sup>+</sup>06] Z. Zhang, S. Sun, X. Zhu, S. Chang, X. Liu, C. Yu, D. Bu, and R. Chen. A novel scoring schema for peptide identification by searching protein sequence databases using tandem mass spectrometry data. *BMC Bioinformatics*, 7(222), 2006.
- [ZWDP09] A.M. Zou, F.X. Wu, J. Ding, and G.G. Poirier. Quality assessment of tandem mass spectra using support vector machine (SVM). *BMC Bioinformatics*, 10(Suppl 1):S49, 2009.